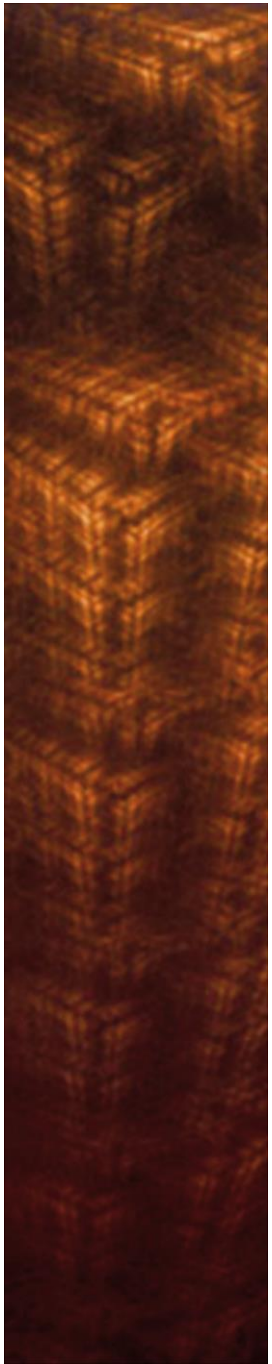

institute IMDEA materials

MULTIFUNCTIONAL NANOCOMPOSITES GROUP

International Workshop on Graphene and Carbon Nanotubes in Experimental Mechanics

University of Manchester, Manchester, UK

Wednesday 15th May 2019

BSSM British Society for Strain Measurement Established 1964

CNT fibres: materials science challenges and perspectives for industrial implementation

Juan J. Vilatela

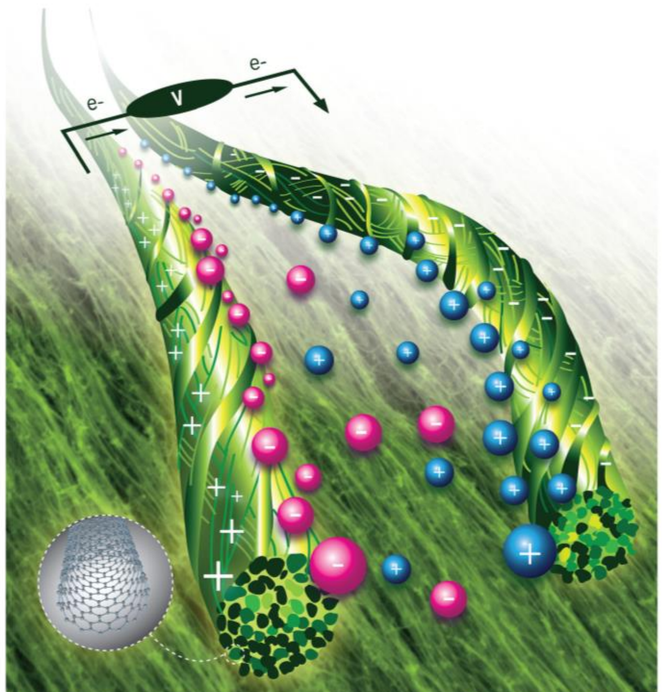

institute IMDEA

500 Researchers

40 Nationalities

A **non-profit research organisation** (foundation) with the **Mission** of doing research of excellence in material science, contributing to tackle the challenges of society and fostering the sustainable development of the region of Madrid.

institute IMdea materials

science transfer talent

science

transfer

talent

Liaoning Jinghua N
ew Material Inc

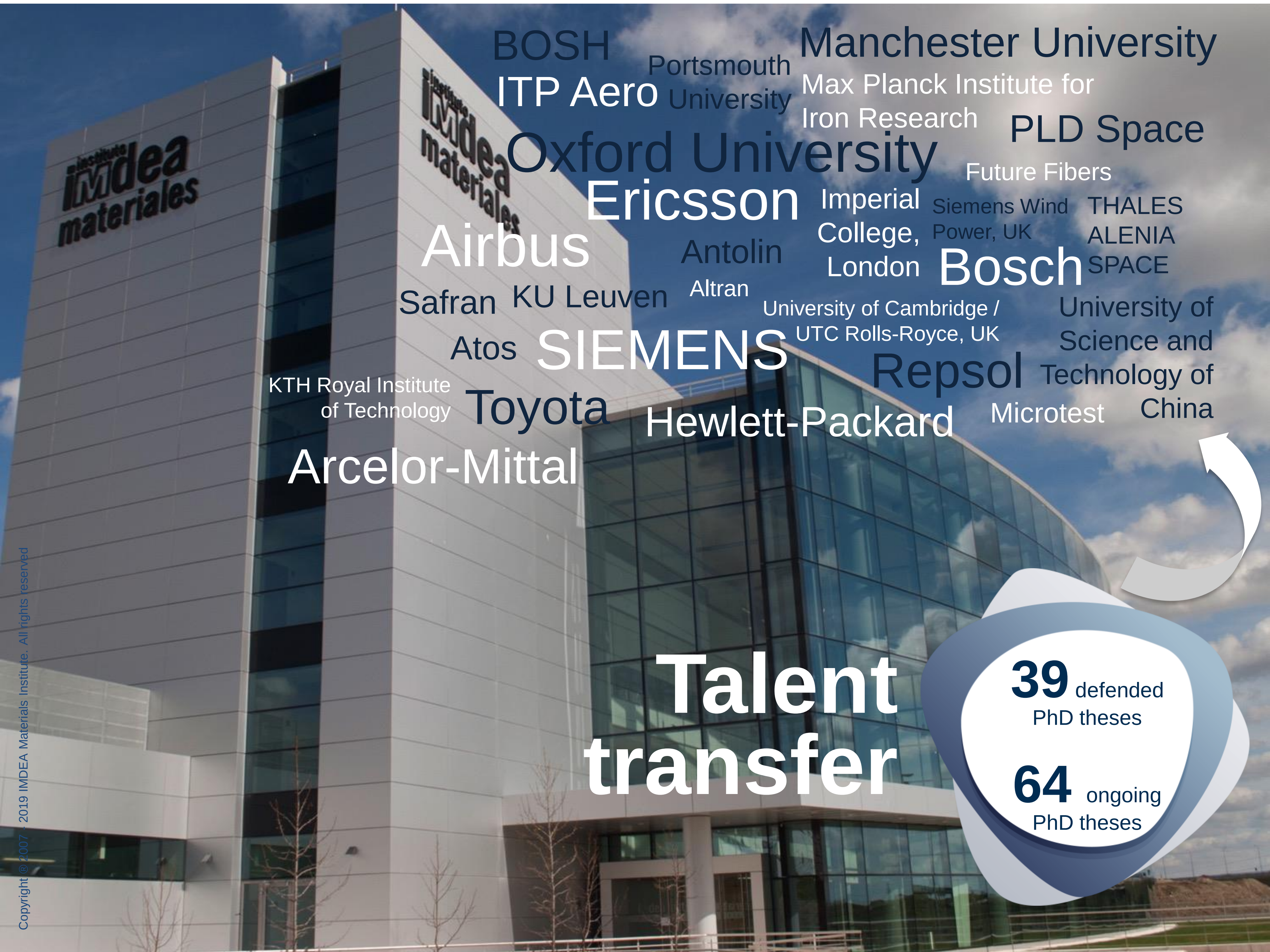
BOSH
Portsmouth University
Manchester University
ITP Aero
Max Planck Institute for Iron Research
PLD Space
Oxford University
Future Fibers
Ericsson
Imperial College, London
Siemens Wind Power, UK
THALES ALENIA SPACE
Airbus
Antolin
Bosch
Safran
KU Leuven
Altran
University of Cambridge / UTC Rolls-Royce, UK
University of Science and Technology of China
Atos
SIEMENS
Repsol
KTH Royal Institute of Technology
Toyota
Hewlett-Packard
Microtest
Arcelor-Mittal
Talent transfer
39 defended PhD theses
64 ongoing PhD theses

Multifunctional nanocomposites group

Synthesis of nanobuilding blocks and assembly into macroscopic structures

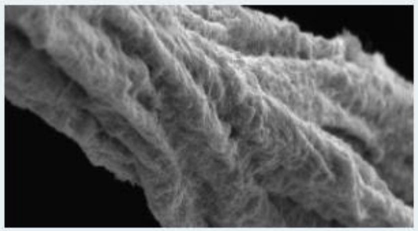

Fabrication and properties of CNT fibre reinforced composites

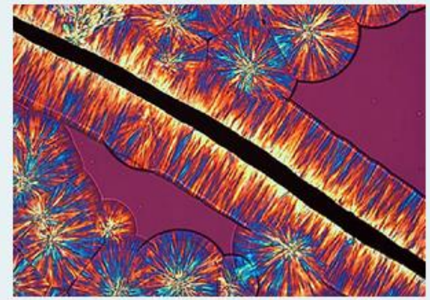

CNT fibre electrochemistry, sensors and energy storage devices

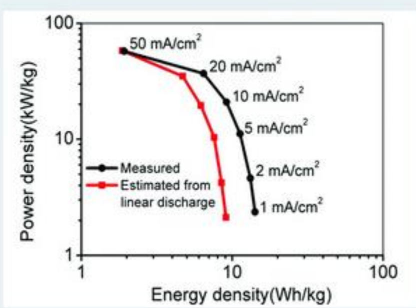

Electronic and photocatalytic properties of CNT-inorganic hybrids

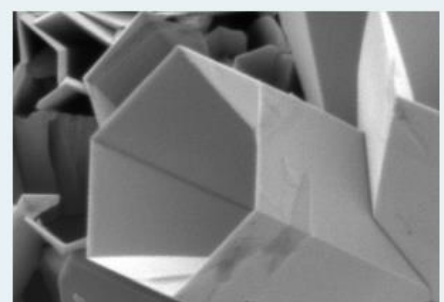

Macroscopic fibres made up of aligned CNTs

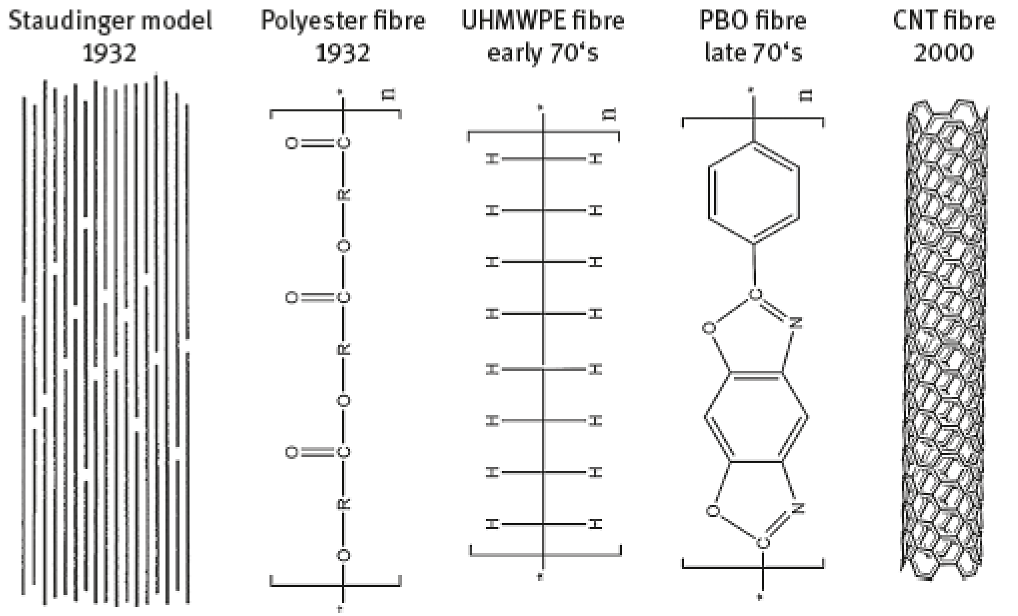

Fig. 8.8: The basic structure of high-performance polymer fibers (Staudinger's model [51]) and some examples of polymers and of a CNT used as building block for synthetic fibers. (Courtesy of H. Yue). With kind permission from Wiley (2006).

Chapter 8, Nanocarbon-Inorganic Hybrids, De Gruyter 2014

Macroscopic fibres made up of aligned CNTs

Tow

Similar to a virus

Single filament

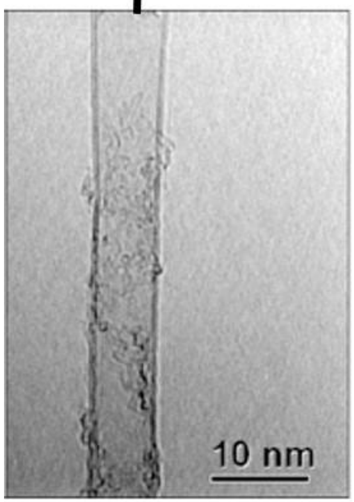

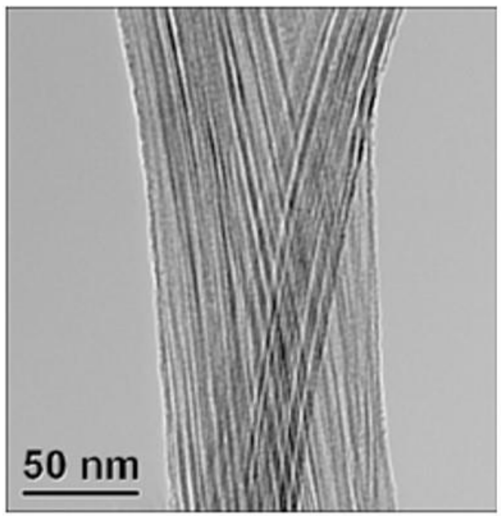

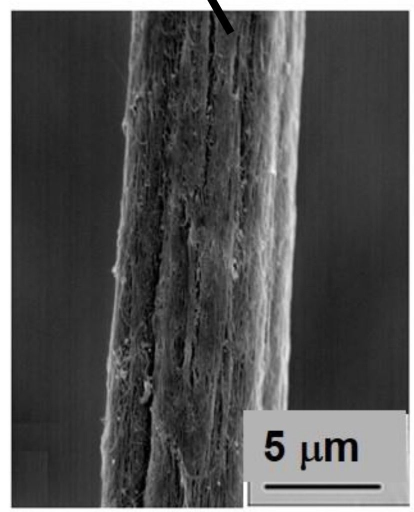

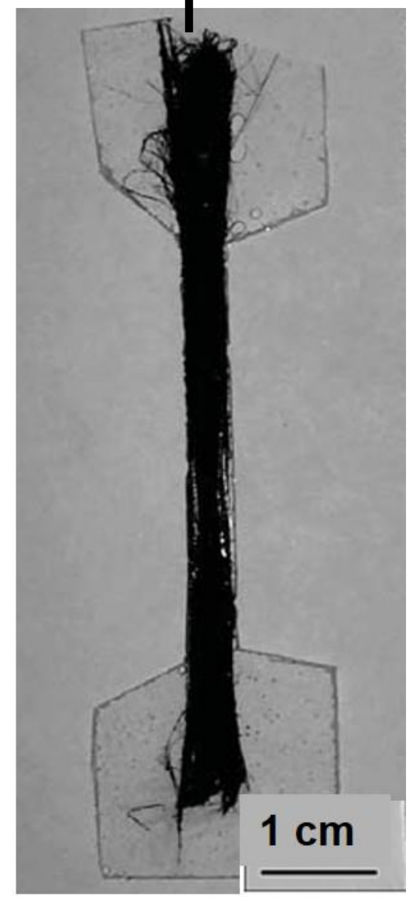

Synthesis of continuous CNT fibres

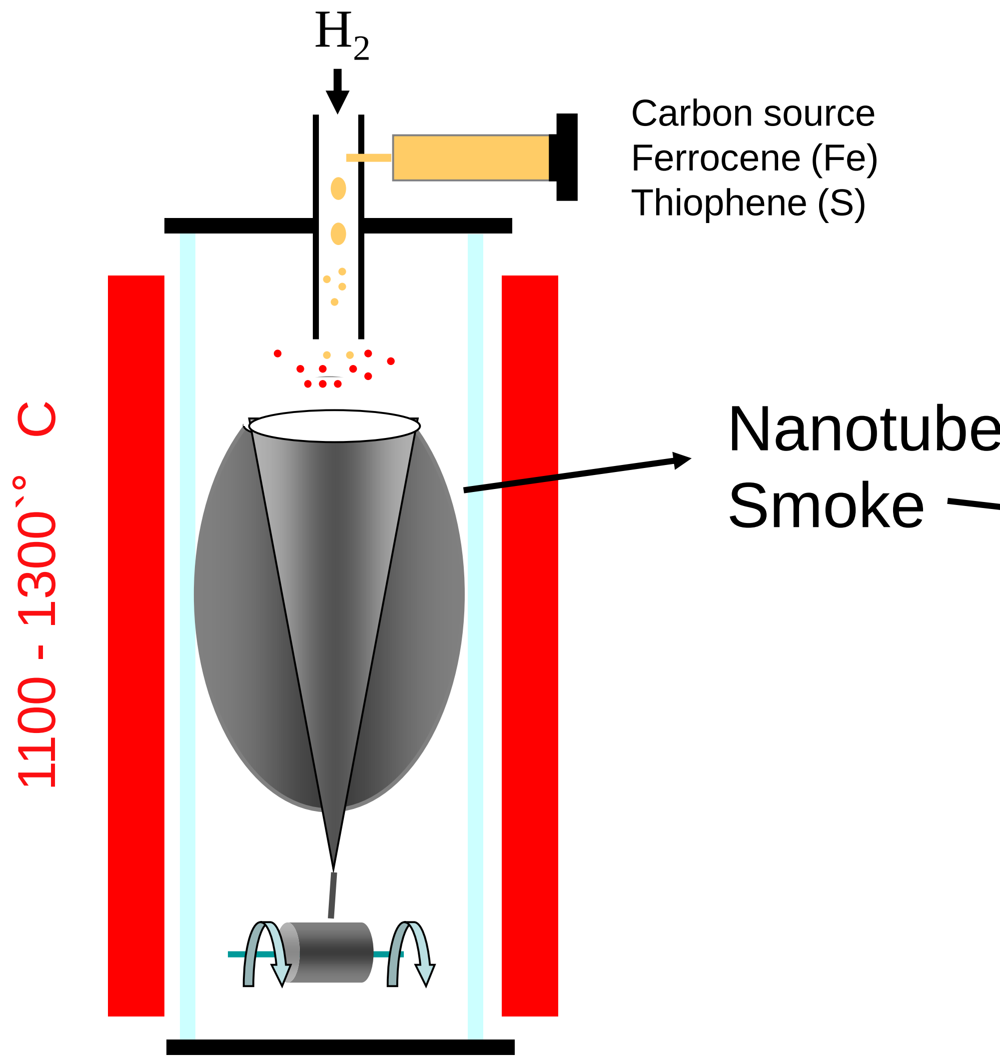

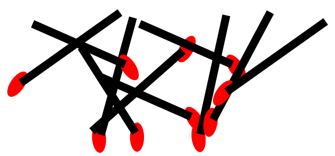

It is elastic!
an aerogel

Courtesy of A. Windle

Ya-Li Li, Ian Kinloch and Alan Windle, *Science*, 304, p 276, 9 April 2004

Floating catalyst CVD

alcohol, S, Fe

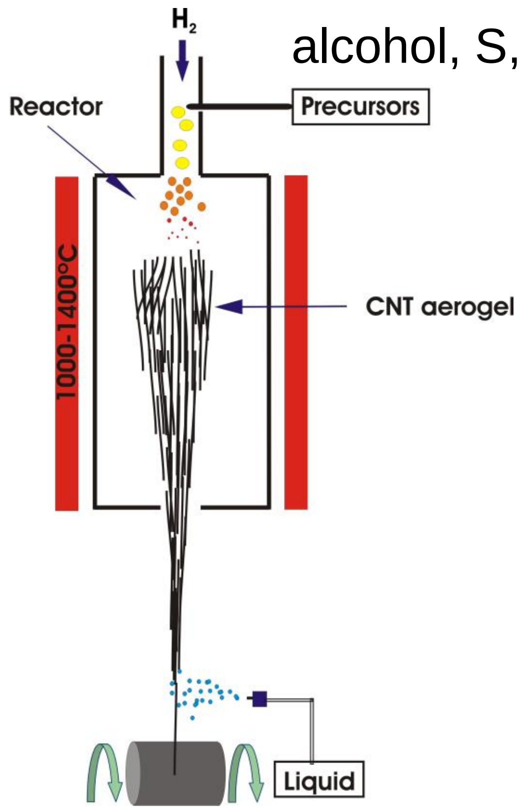

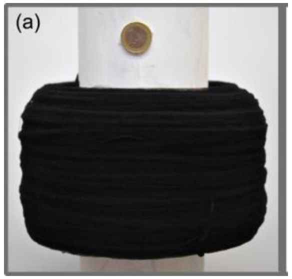

Reguero et al, Chem Mater, 26, 3550 2014

Looking up into the reactor

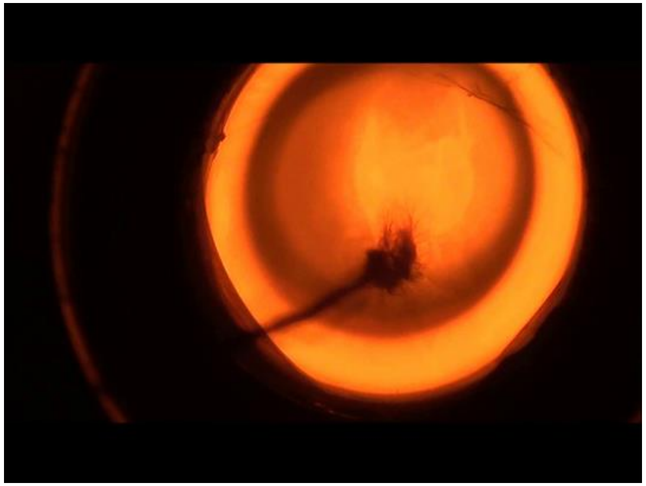

Continuous spinning of 1km

A macroscopic fibre made of carbon nanotubes

alcohol, S, Fe

Looking up into the reactor

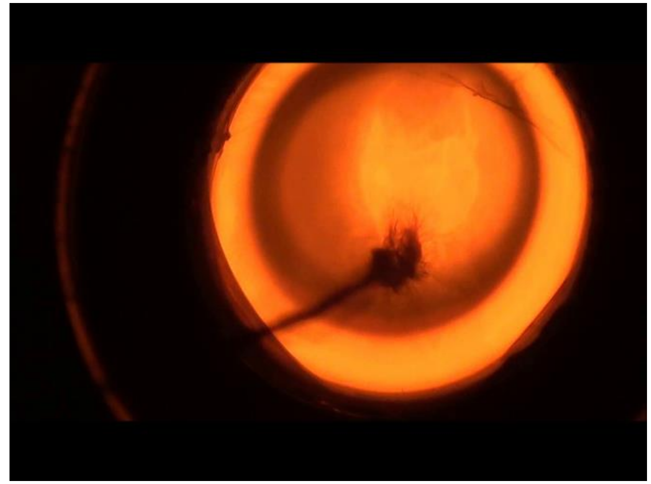

Continuous spinning of 1km

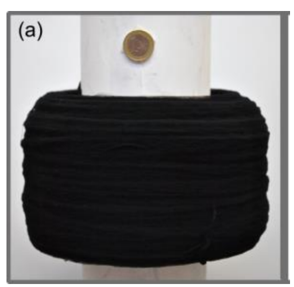

Reguero et al, Chem Mater, 26, 3550 2014

A macroscopic fibre made of carbon nanotubes

Looking up into the reactor

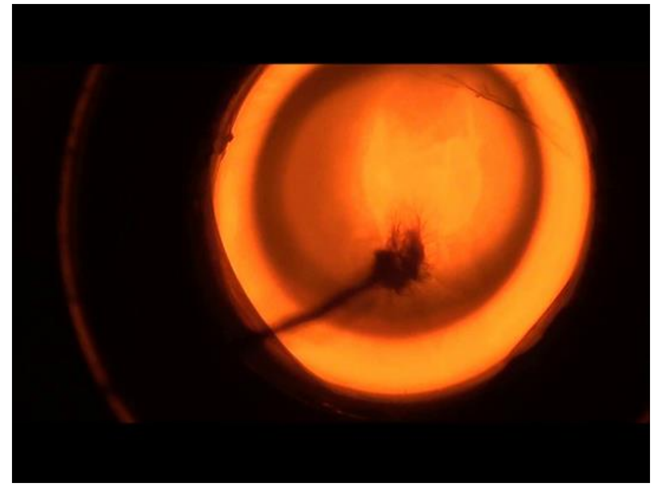

Continuous spinning of 1km

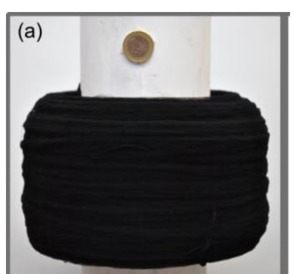

Reguero et al, Chem Mater, 26, 3550 2014

CNT type and fibre alignment be controlled

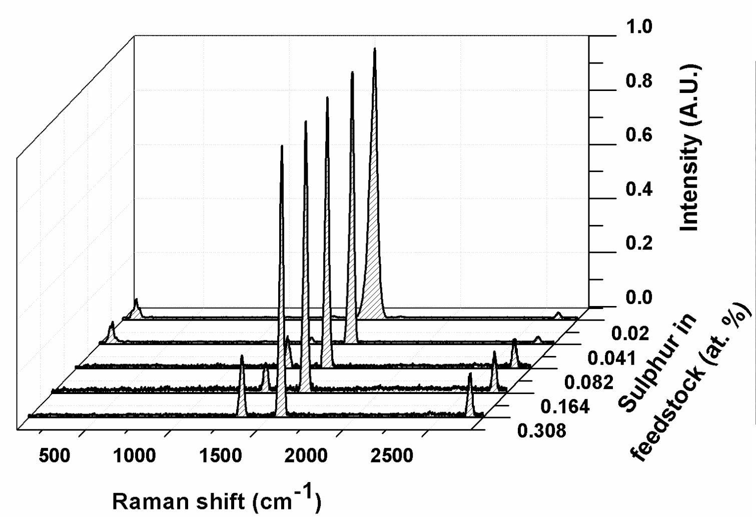

Layers controlled through S/C ratio

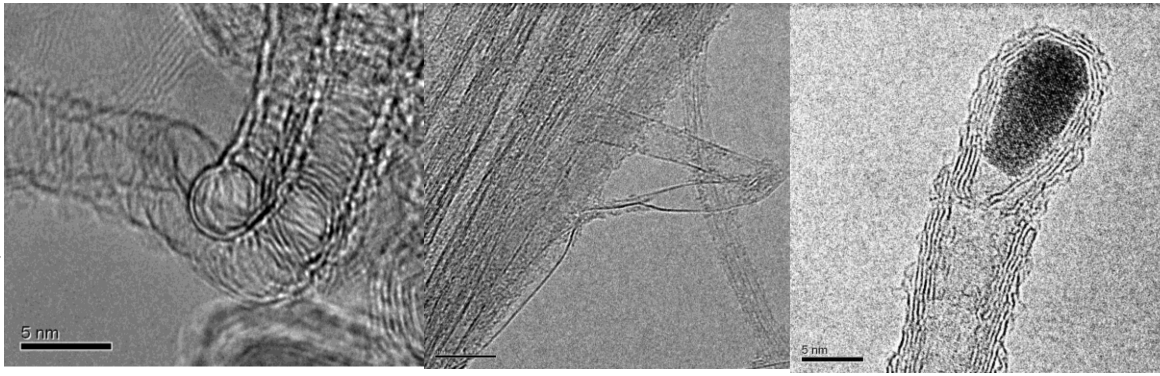

Reguero et al, Chem Mater, 26, 3550 2014

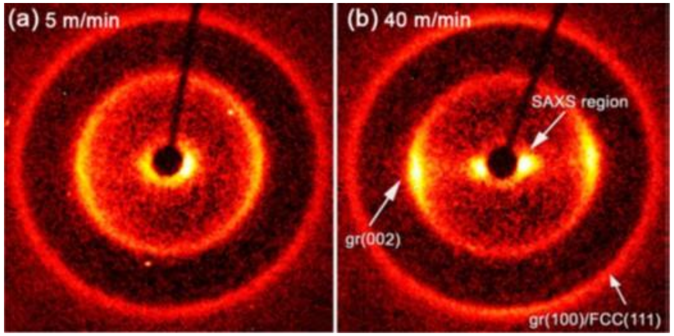

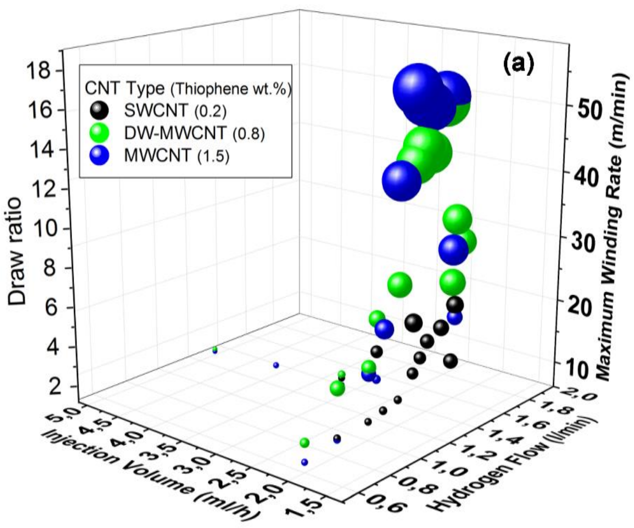

Aleman et al, ACS Nano, 9, 7392, 2015

Scale up efforts around the world

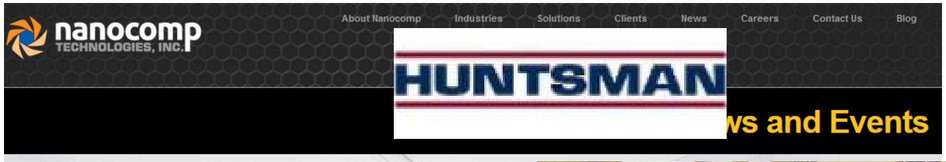

Technologies

June 6,2014 – Nanocomp
t to celebrate the expansio
e. The company is tripling
g - in the upcoming year. U
Maggie Hassan, will be pre
on and its impact on the m
olice Departments will be p

Core Conductor for Data Transmission

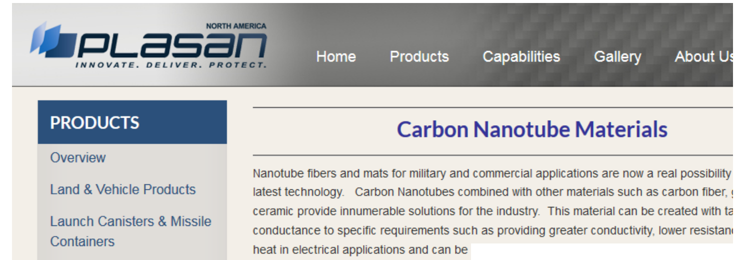

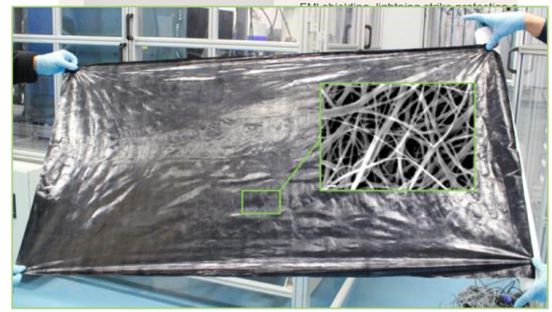

SYNANO

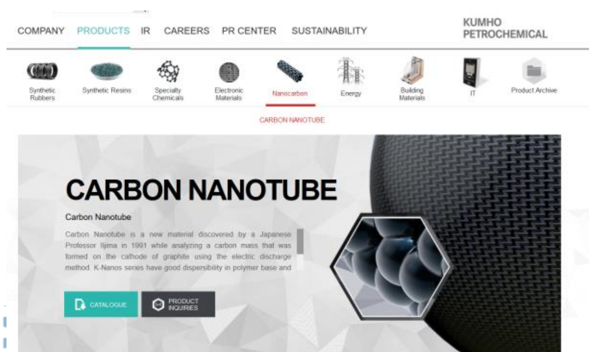

LG Chem

INFRA
GTL TECHNOLOGY

Different CNT fibre formats

Single filament

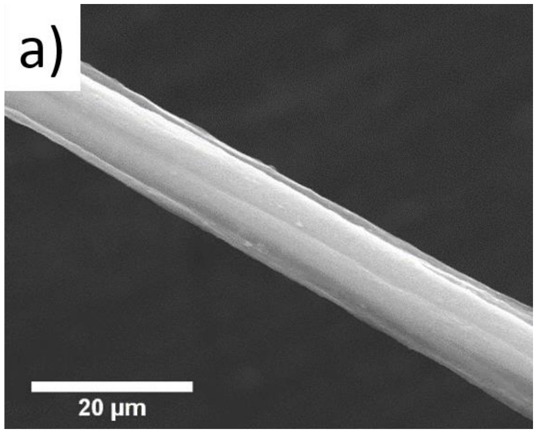

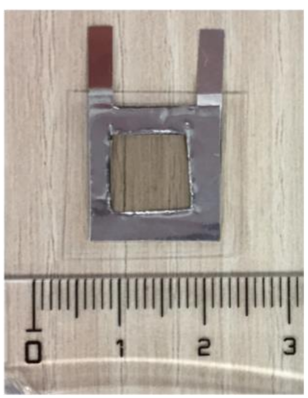

- Transparent conductor
- Microelectrode

Yarns (10-100 filament tow)

- Electrical conductor
- Electrode
- Sensor

Unidirectional sheets

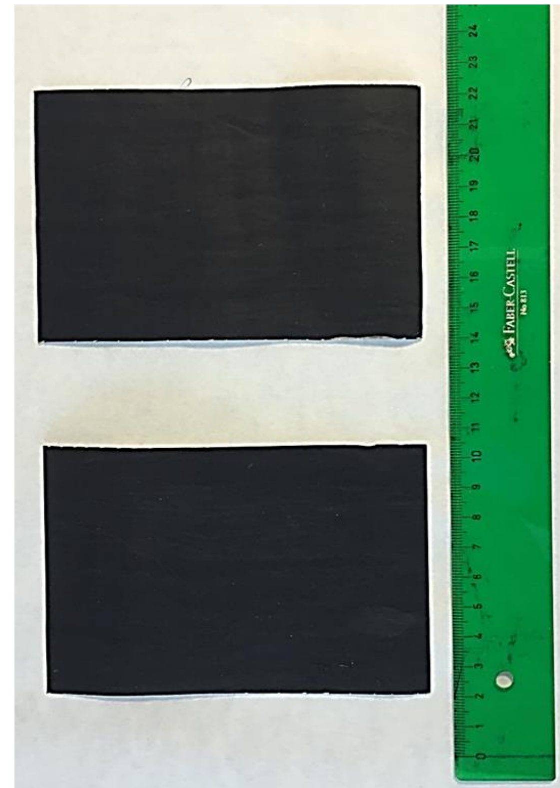

- Electrode/current collector
- Laminate composite reinforcement

A fundamentally different type of carbon material

CNT Fibre

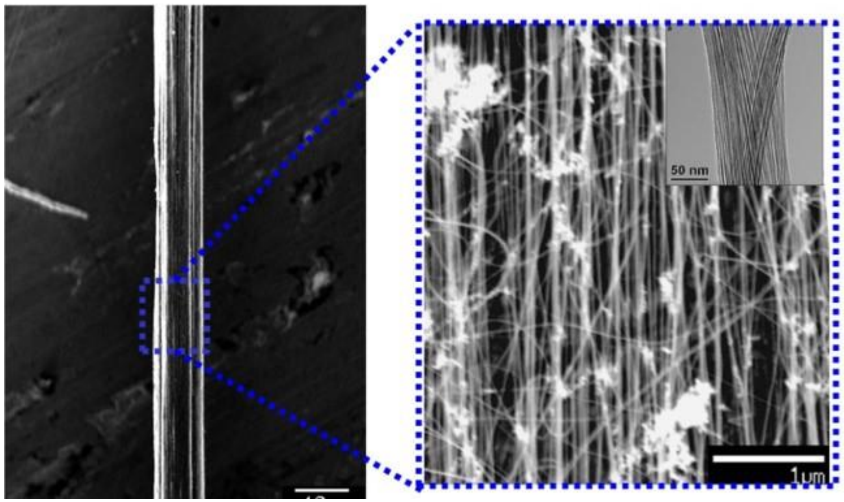

Conductivity 10^3 S/cm

Carbon Fibre

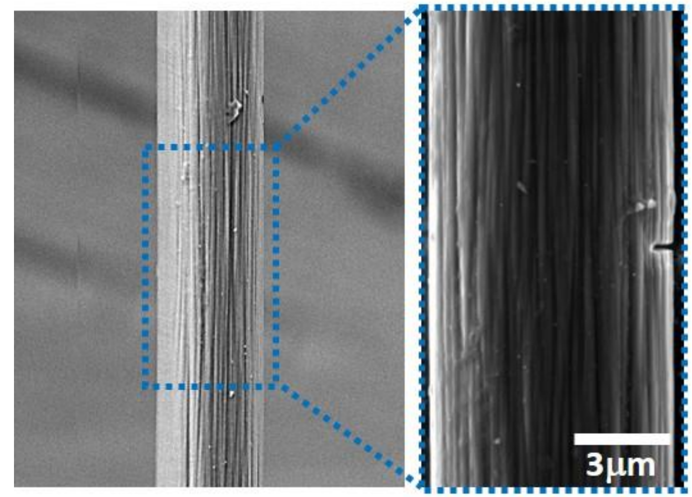

10^2 S/cm

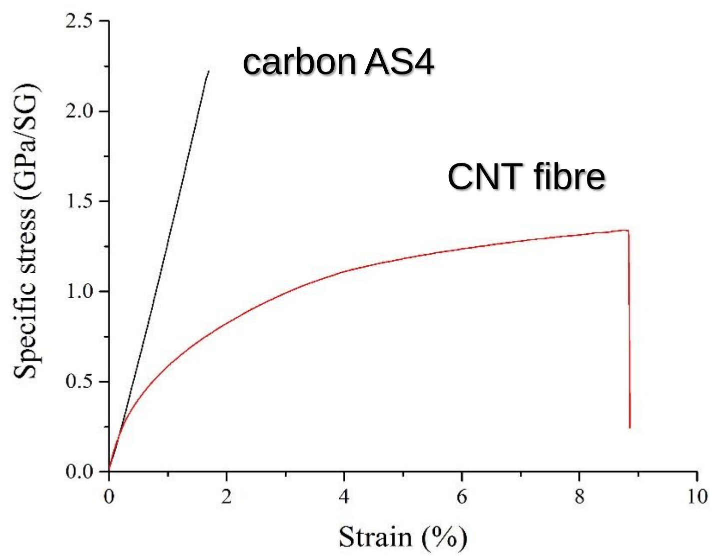

Current fibre properties

Mechanical

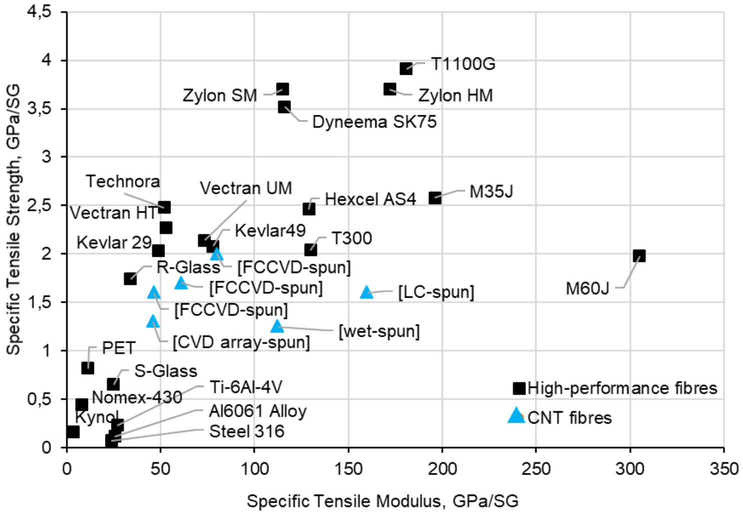

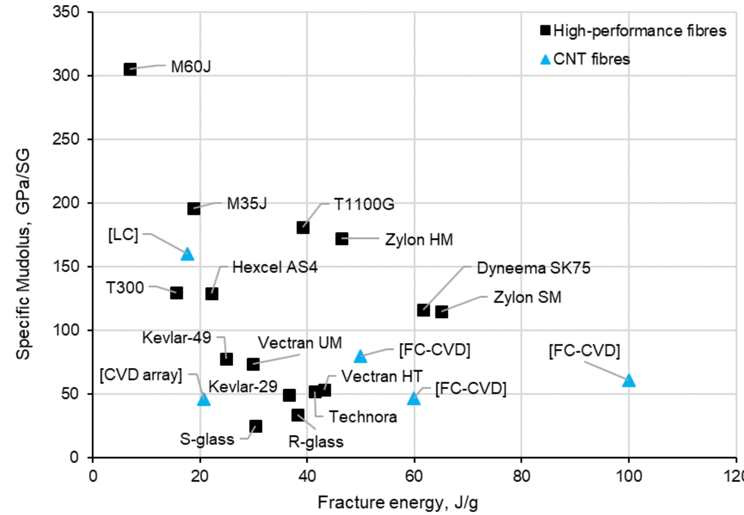

A Perspective on High-performance CNT fibres for Structural Composites; Carbon; 150, 191, 2019;

Mechanical/electrical

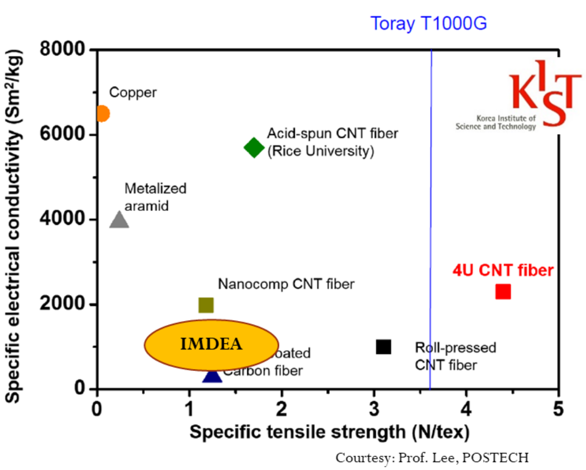

Electrochemical/mechanical

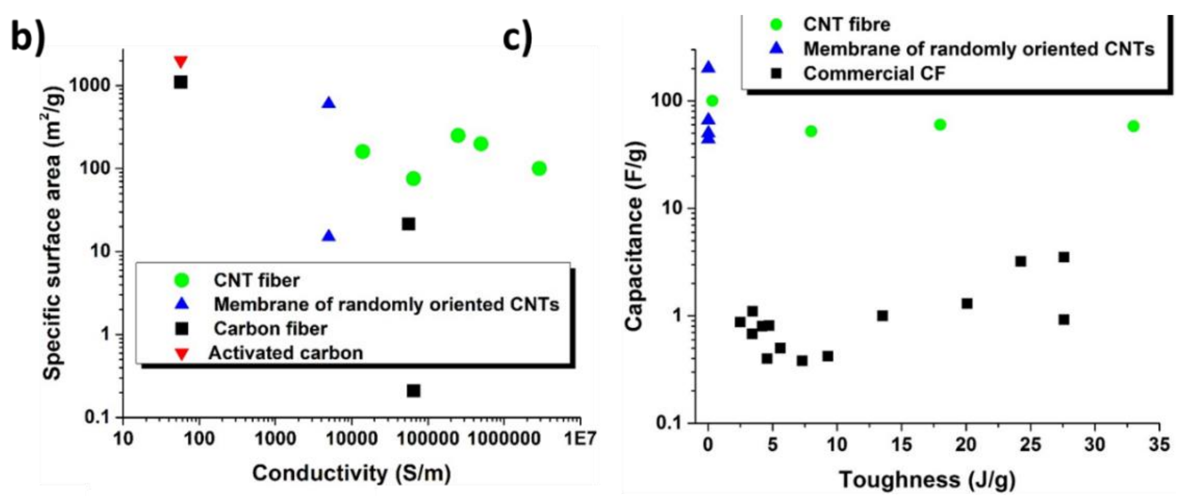

CNT fibres as macromolecular systems

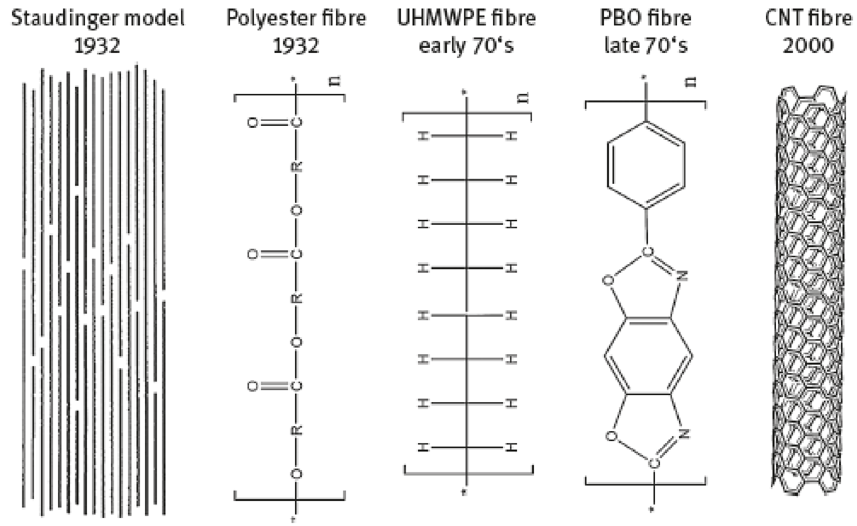

Chapter 8, Nanocarbon-Inorganic Hybrids, De Gruyter 2014

UHMWPE fibre

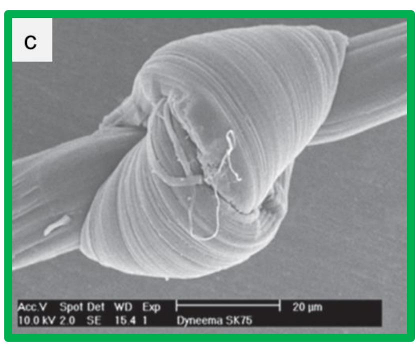

CNT fibre

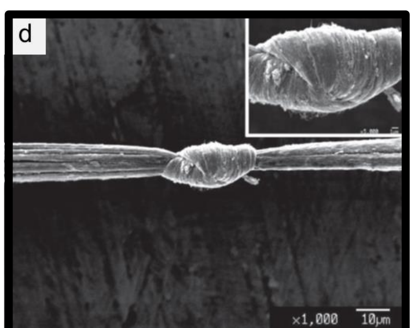

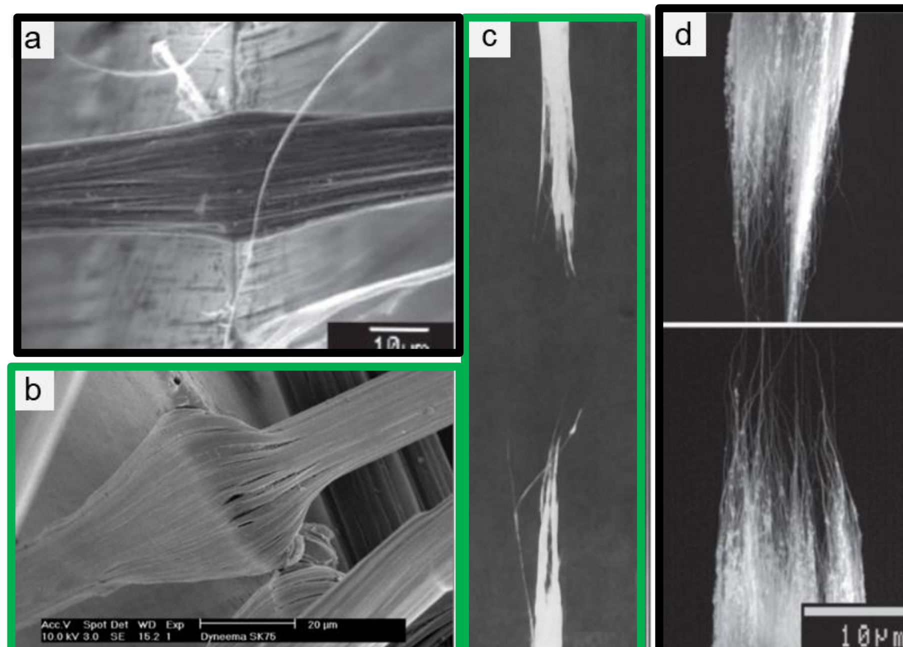

Structure – tensile properties

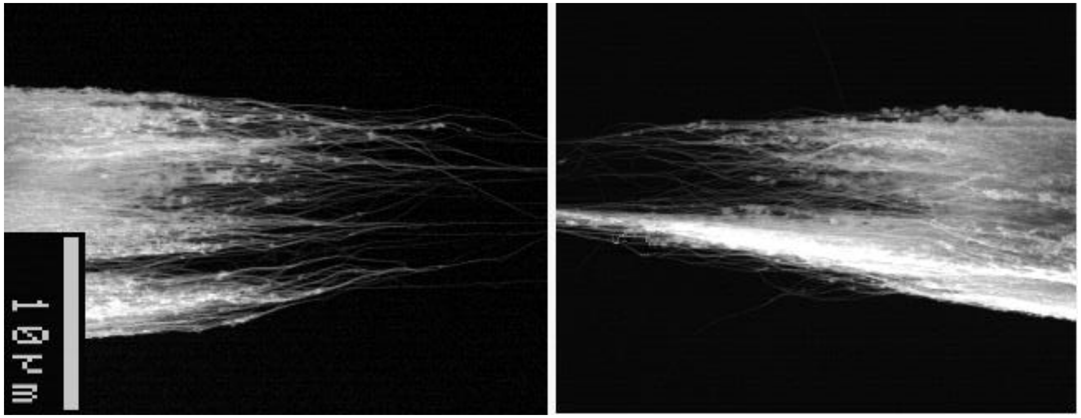

Vilatela, Elliott, Windle, ACS Nano, 2011

Shear strength (30kPa)

$$\sigma' = \frac{1}{6}\Omega_1\Omega_2\tau_F L$$

CNT laterlal overlap

CNT length (1mm)

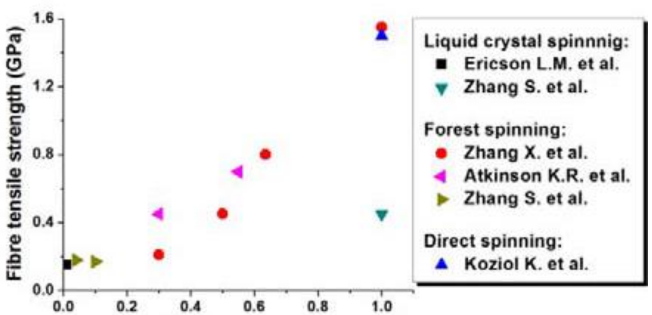

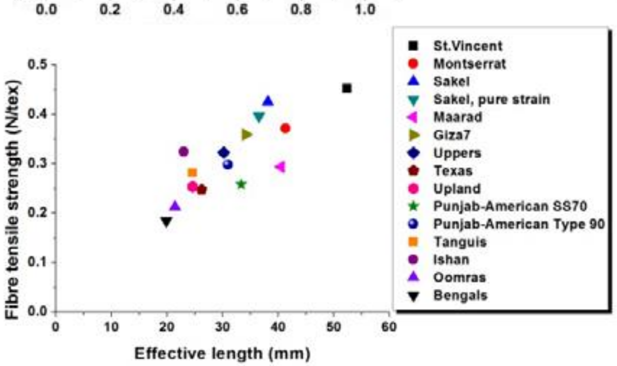

J. Eng. Fibers and Fabrics. 2013

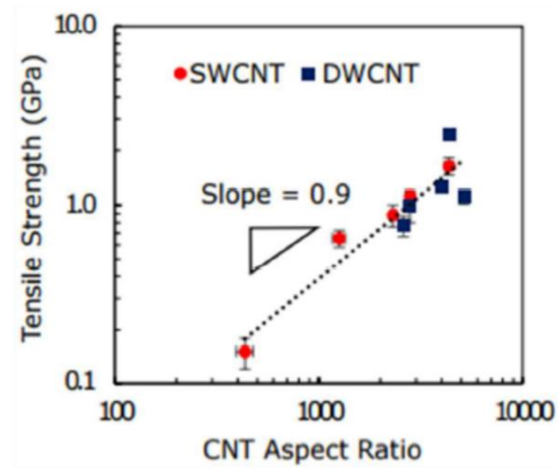

Tsentalovich, et al.. ACS Appl Mater Interfaces 2017; 9:36189–36198

The uniform stress transfer model

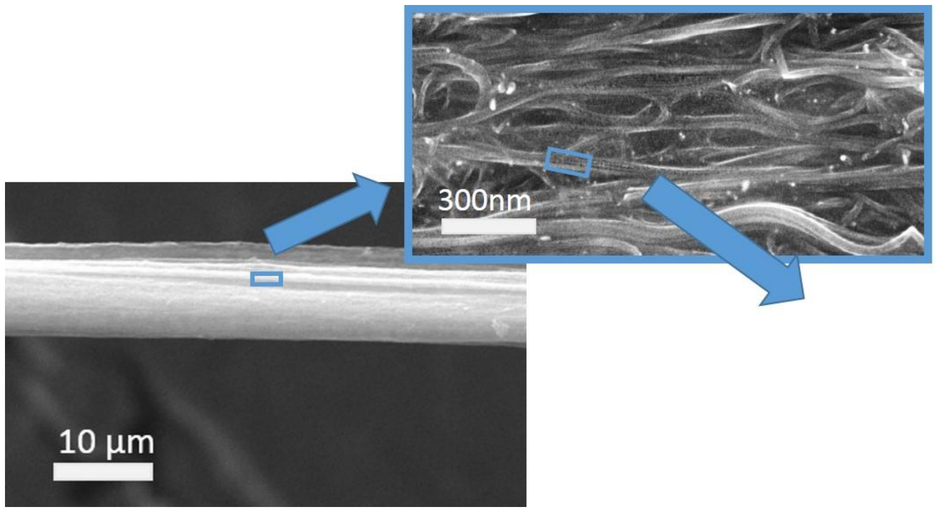

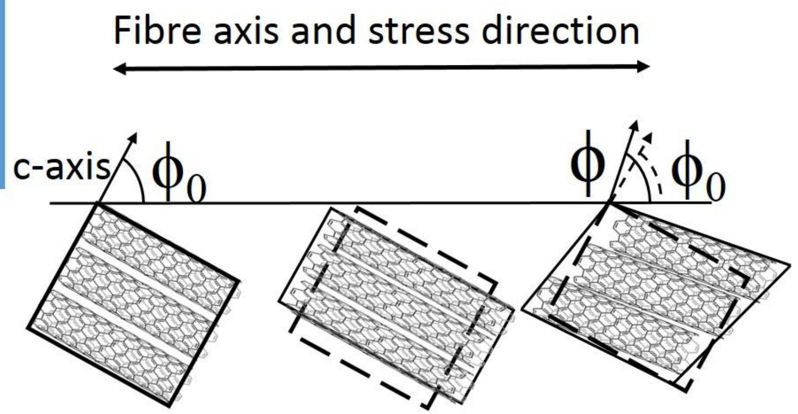

- The fibre is reduced to a network of bundles
- Deformation through bundle stretching and shear
- Only for highly aligned systems: $\langle sin\phi_0\rangle \approx 1, \langle cos^4\phi_0\rangle \ll \langle cos^4\phi_0\rangle$

$$\frac{1}{E} = \frac{1}{e_c} + \frac{<\cos^2(\phi_0)>}{g}$$

$$<\cos^2(\phi_0)> = \frac{\int_0^{\pi} \cos^2(\phi_0) I(\phi_0)\sin(\phi_0)d\phi}{\int_0^{\pi} I(\phi_0)\sin(\phi_0)d\phi}$$

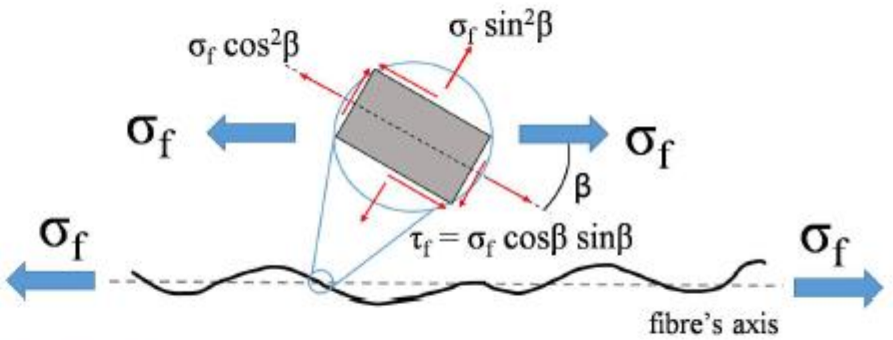

Fig. 5.4 Illustration of the state of stresses for a structural elements into the fibre according to the uniform stress model.

Fernández-Toribio et al, Carbon, 133, 44, 2018

Experimental study

Samples with different alignment

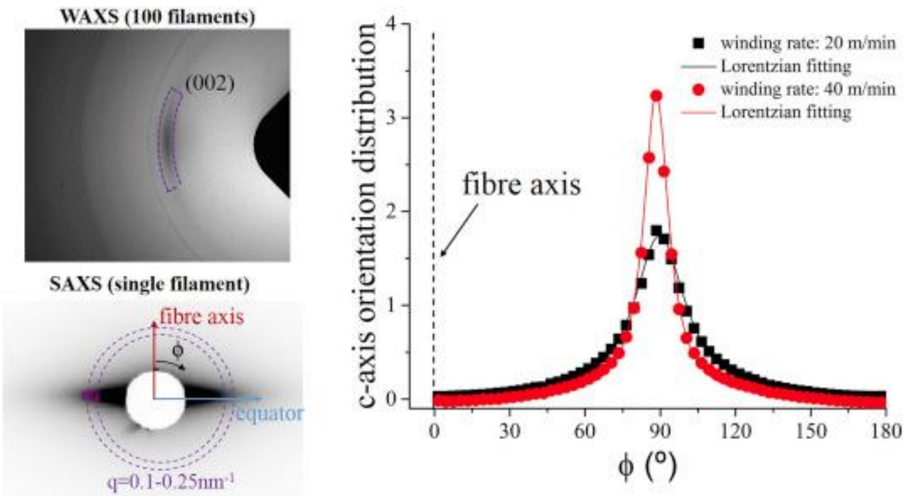

ODF from the form factor in SAXS

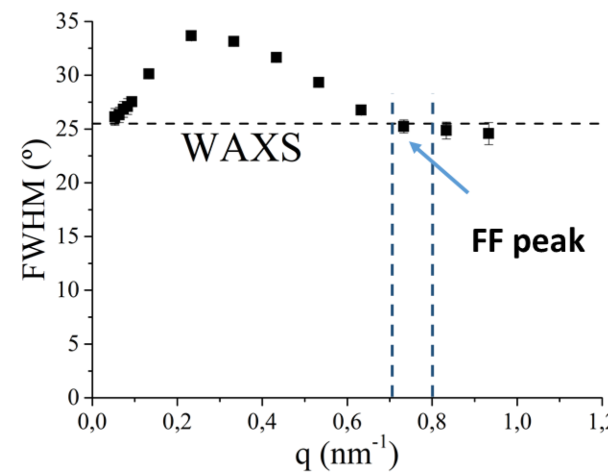

Table 1: Experimental values of CNT fibres

	winding rate (m/min)	$< cos^2\phi_0 >$ ($\times 10^{-2}$)	E (GPa)	σ_b (GPa)	Fracture energy (J/g)
Collapsed DWNTs	4	8.89	44 ± 9	1.0 ± 0.2	70 ± 40
	8	9.7	32 ± 7	1.1 ± 0.1	90 ± 20
	12	7.46	56 ± 8	1.3 ± 0.2	70 ± 30
	16	5.42	61 ± 7	1.7 ± 0.3	100 ± 30
Few-layer MWNTs	20	11.58	33 ± 8	0.7 ± 0.1	60 ± 10
	30	10.08	38 ± 8	0.8 ± 0.1	65 ± 15
	40	6.37	64 ± 16	1.1 ± 0.2	80 ± 40

2 batches of different CNT type

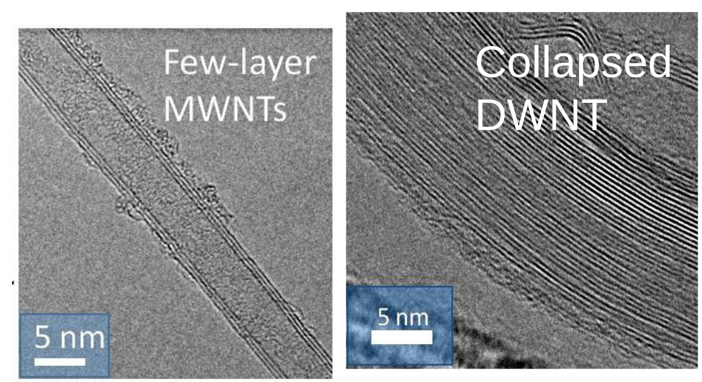

Fernández-Toribio et al, Carbon, 133, 44, 2018

Successful fitting of experimental data

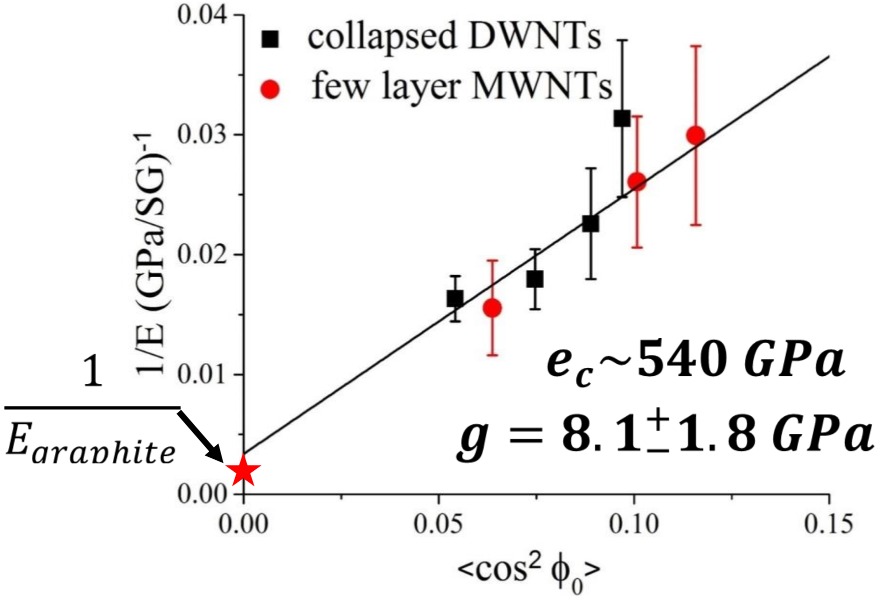

$$\frac{1}{E} = \frac{1}{e_c} + \frac{<\cos^2(\phi_0)>}{g}$$

The stiffness of CNT fibres is mainly dominated by the ODF of nanotubes

Fernández-Toribio et al, Carbon, 133, 44, 2018

A general description of aligned CNT fibres

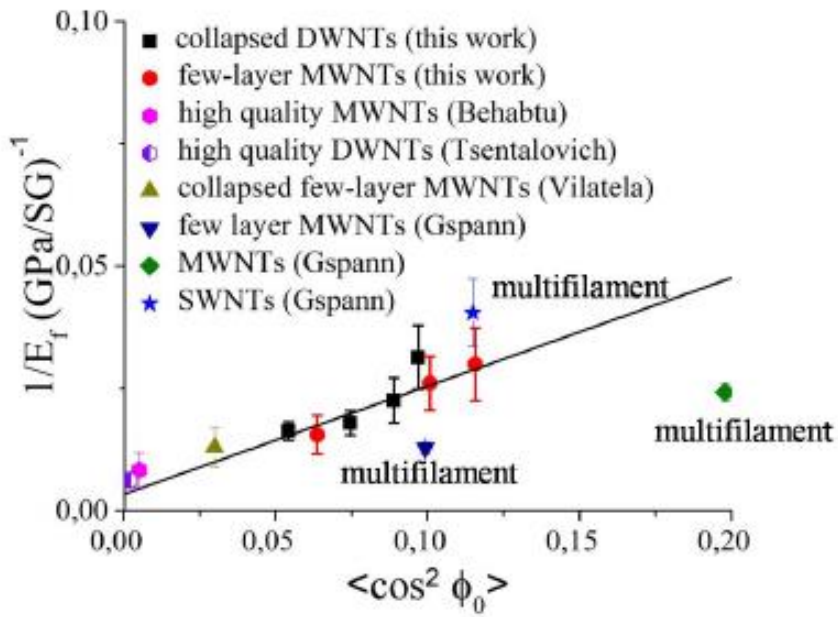

Data for CF

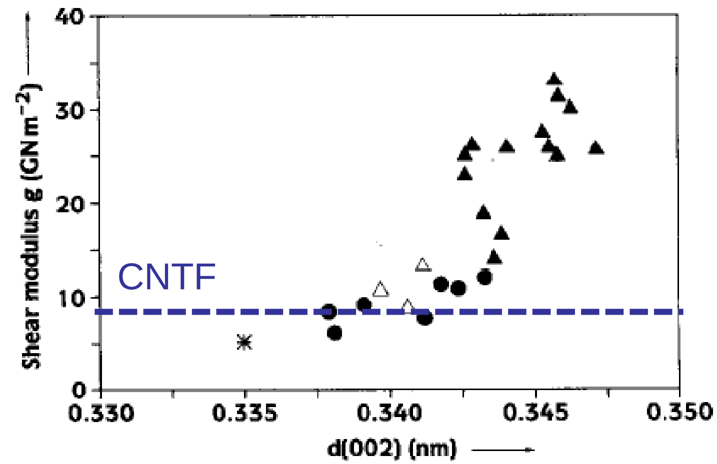

Fig. 8. Shear modulus g as a function of the lattice spacing $d(002)$. Graphite is indicated by (*).

Northol et al, Carbon, 29, 1991

$$\frac{1}{E} = \frac{1}{e_c} + \frac{<\cos^2(\phi_0)>}{g}$$

The model successfully describes the elastic properties of aligned CNT fibres

Fernández-Toribio et al, Carbon, 133, 44, 2018

Uniform stress transfer and Raman

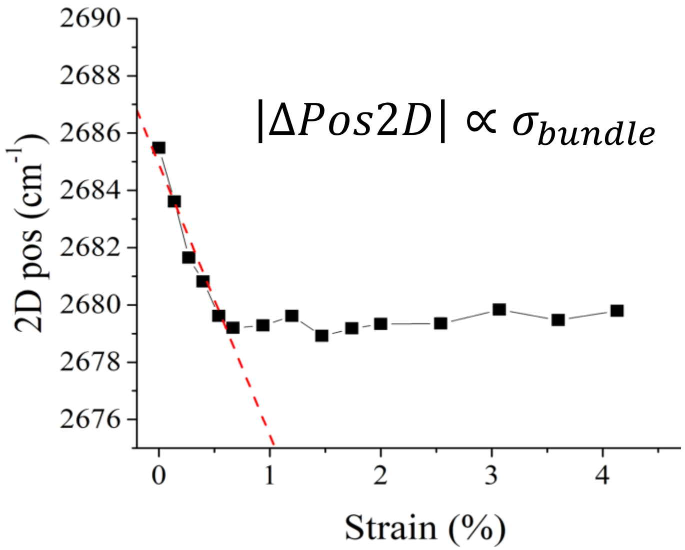

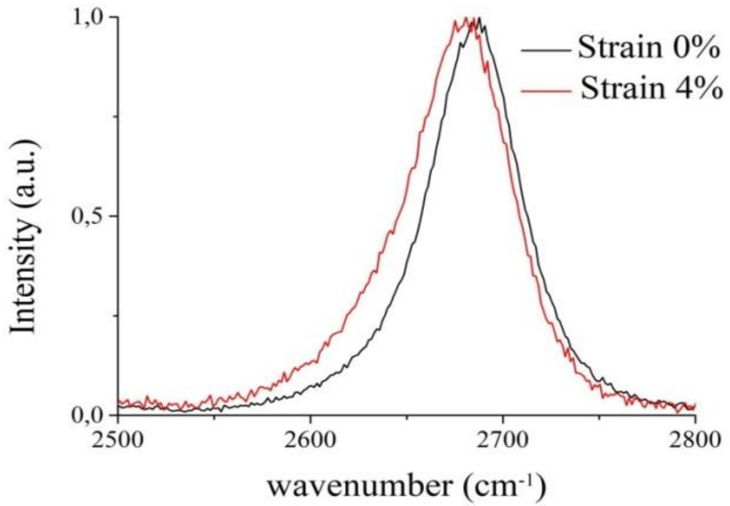

$$\frac{|\Delta Pos2D|}{\Delta\varepsilon_f} \propto \frac{\sigma_f}{\varepsilon_f} = E_f$$

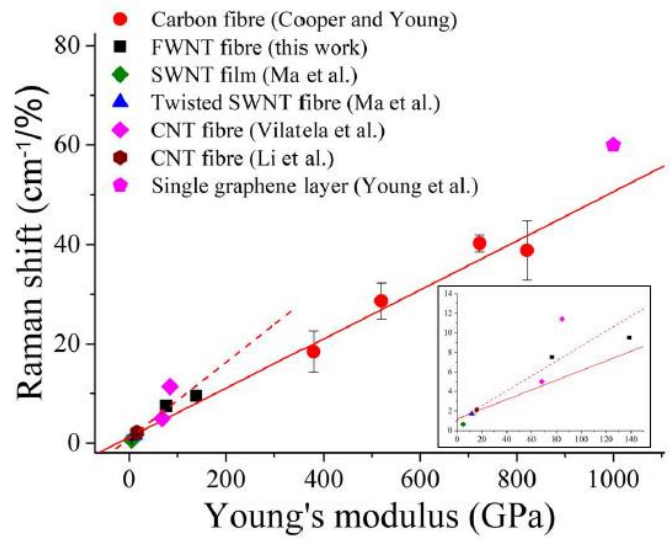

The change in stress state of a bundle
(measured by Raman) per bulk strain,
is proportional to the fibre bulk longitudinal modulus

Tensile properties and fracture energy

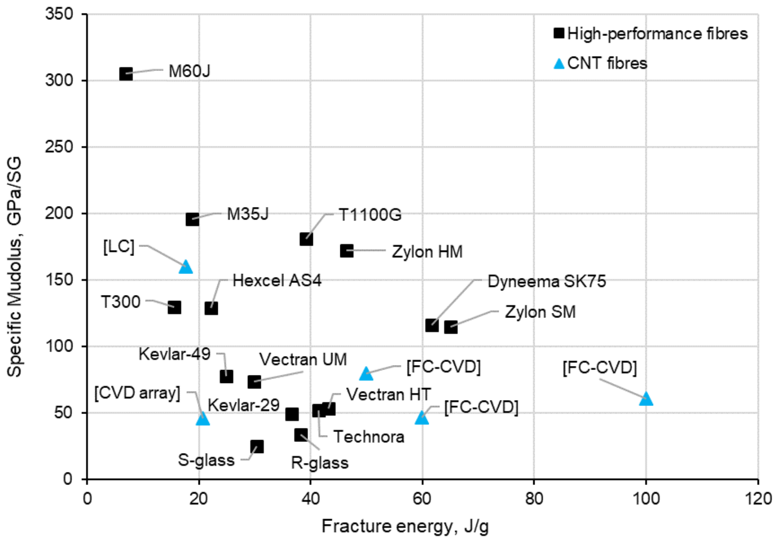

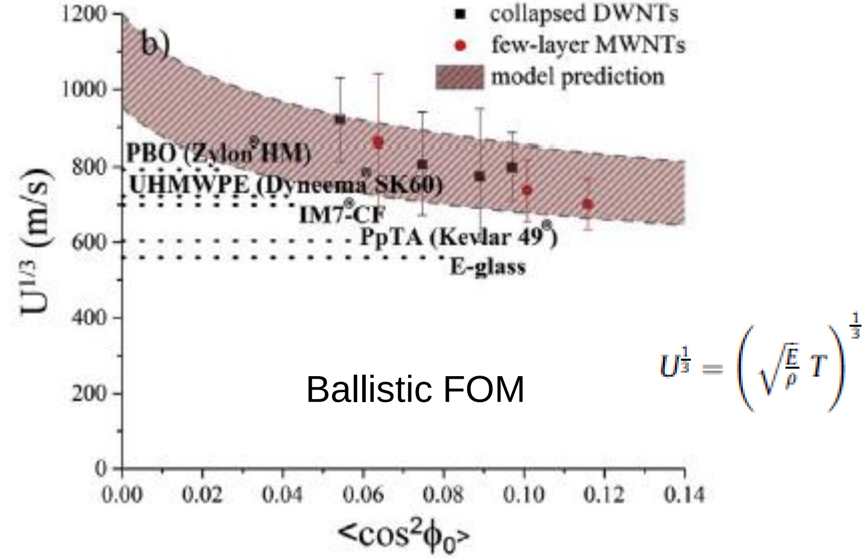

Unusual elastoplastic deformation

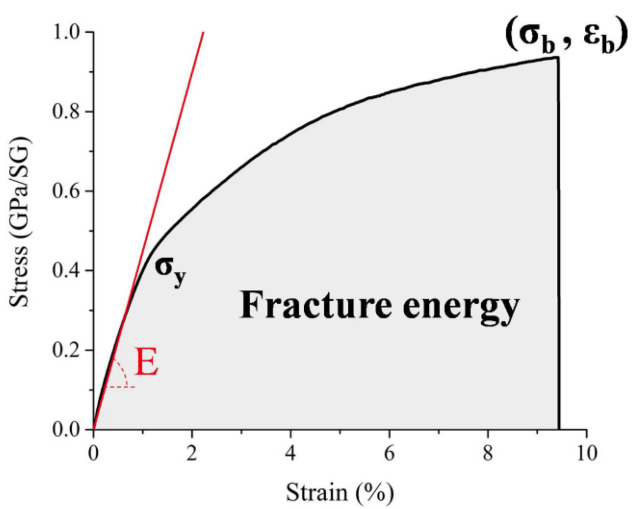

Strain-hardening

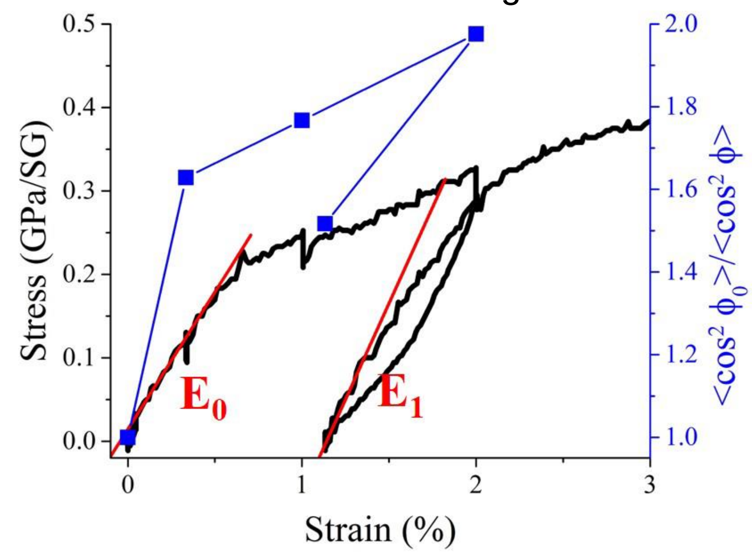

Monitoring alignment evolution during stretching

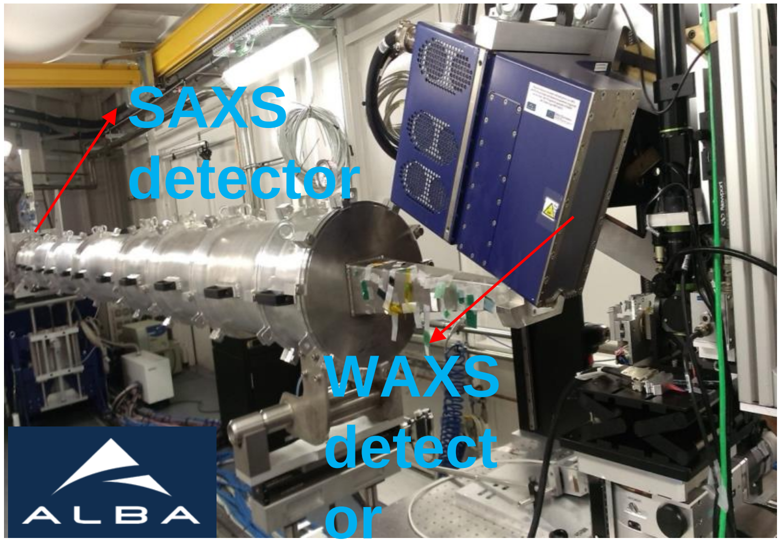

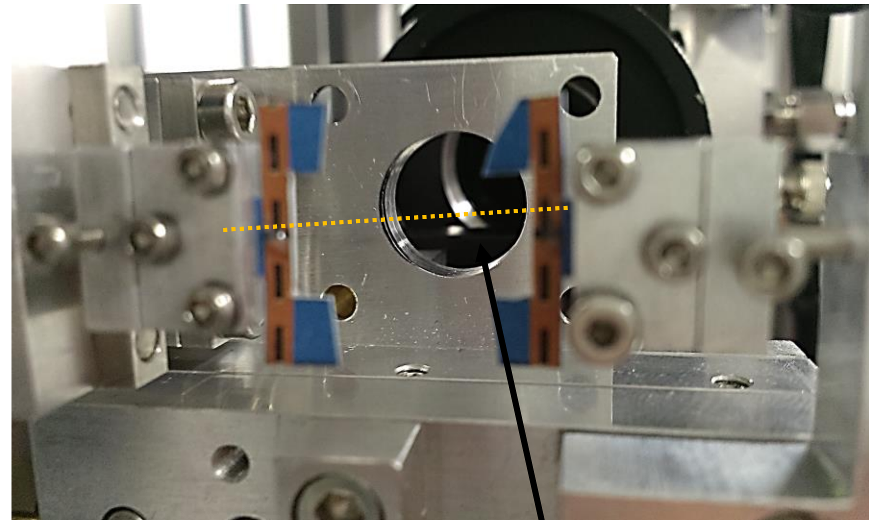

10-micron diameter filament

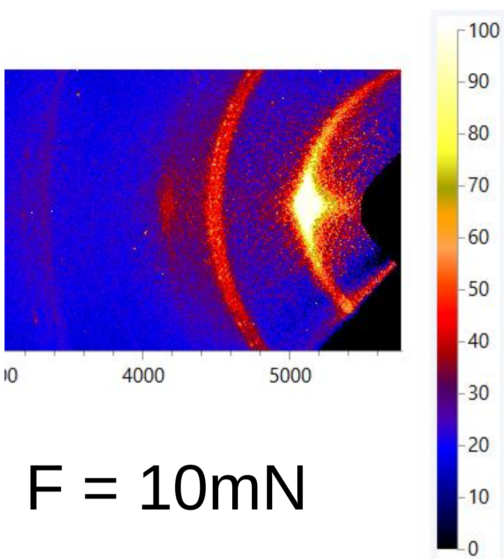

F = 10mN

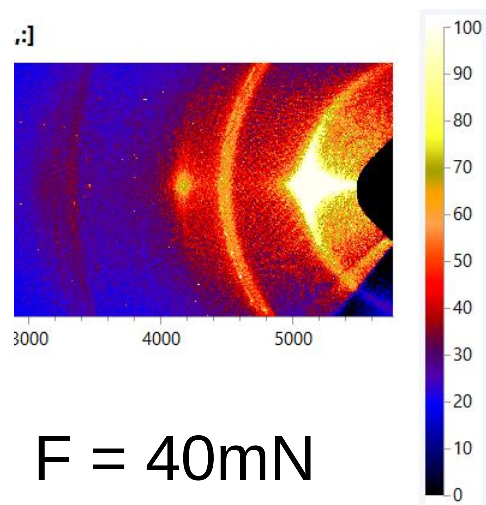

F = 40mN

Radial profiles – mesoscopic structural changes

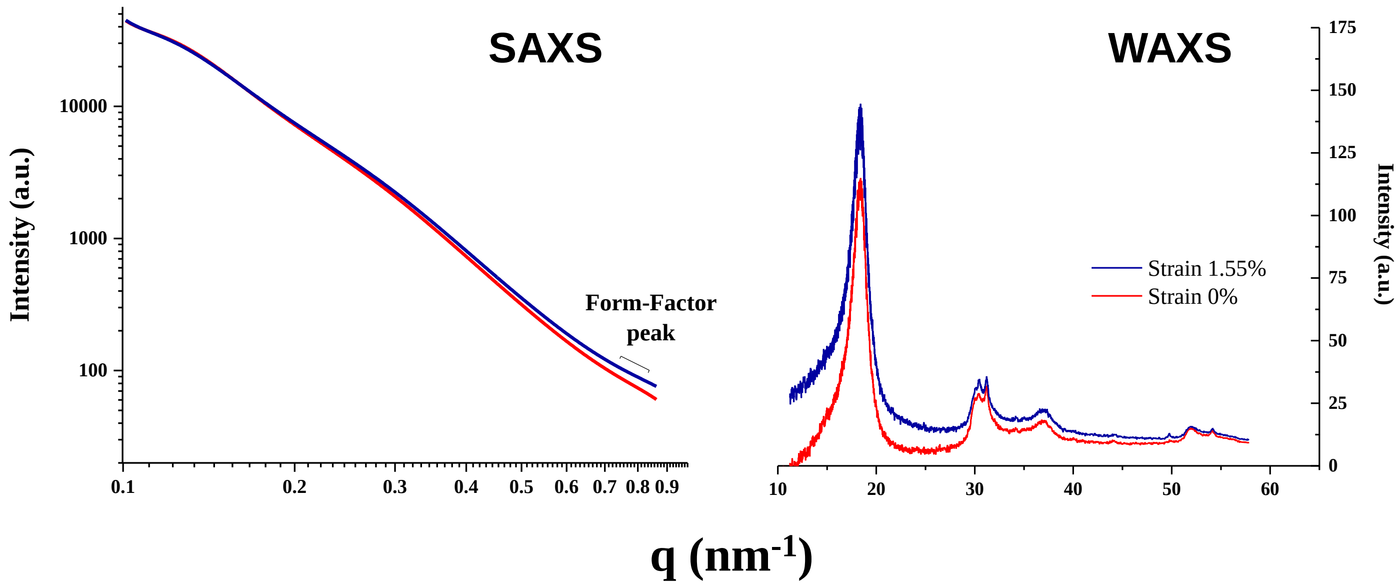

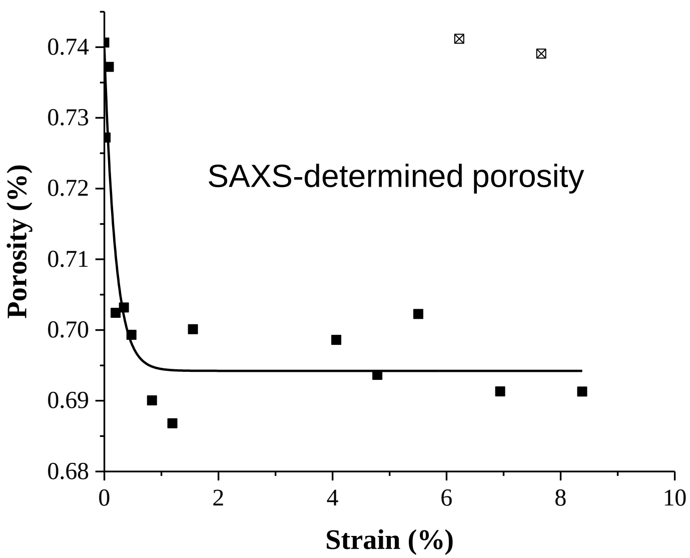

Main observations:

- Structural changes are in micro-pore structure
- No formation of turbostratic domains (stretch-crystallisation)

A description of the elastoplastic deformation

U: strain alignment

$$U = \frac{< \cos^2 \phi_0 >}{< \cos^2 \phi >} - 1$$

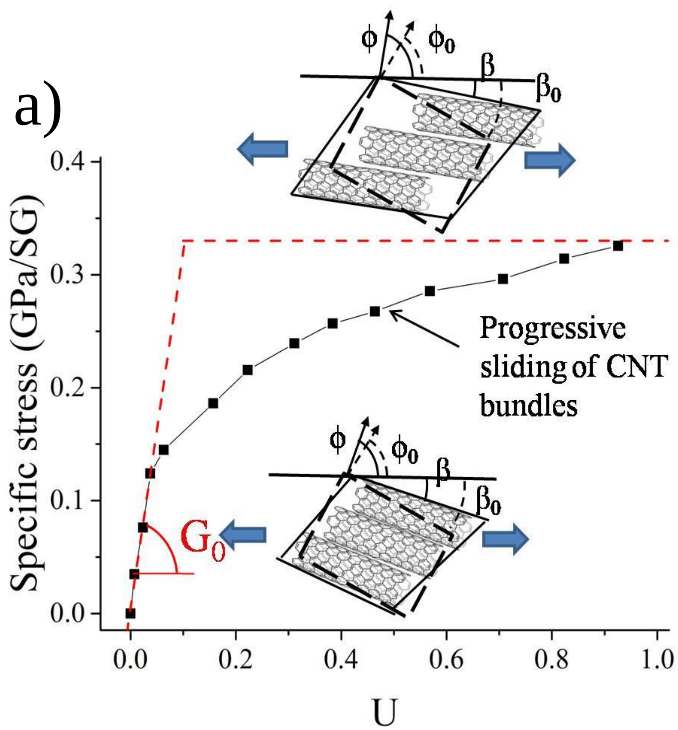

From continuum mechanics

$$< \cos^2 \phi > = < \cos^2 \phi_0 > \cdot \exp(-\frac{\sigma}{g})$$

Northol et al., Polymer, 21, 1199

$$\frac{< \cos^2 \phi_0 >}{< \cos^2 \phi >} = \exp(\frac{\sigma}{g}) \approx 1 + \frac{\sigma}{g}$$

$$G = \frac{\Delta U}{\Delta \sigma}$$

$$\sigma = g \cdot U$$

The monotonic decrease in G is due to progressive sliding ot CNT bundles (at different stress levels)

Fernández-Toribio et al, in preparation

Elastoplastic deformation

$$P_f = 1 - \frac{G}{G_0}$$

$$P_f = 1 - \exp\left[-\left(\frac{\sigma}{\sigma_{0b}}\right)^m\right]$$

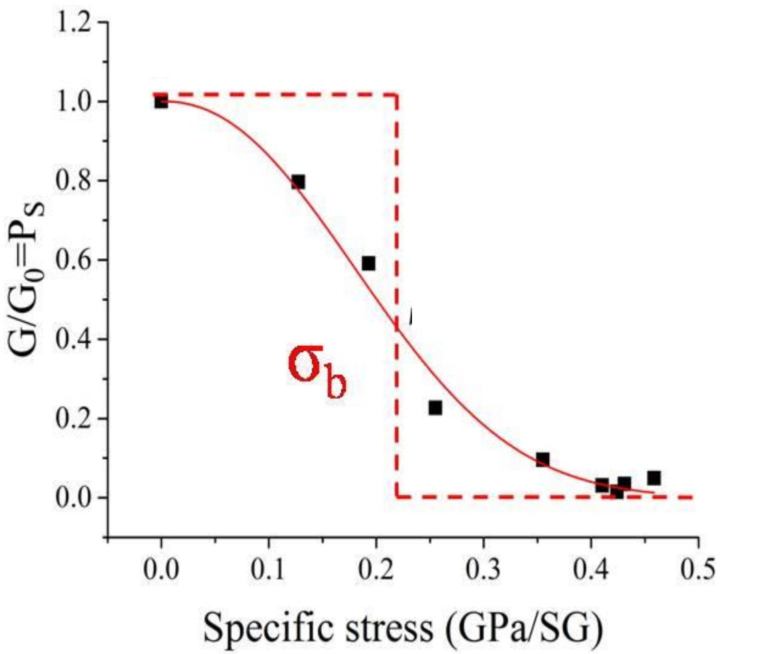

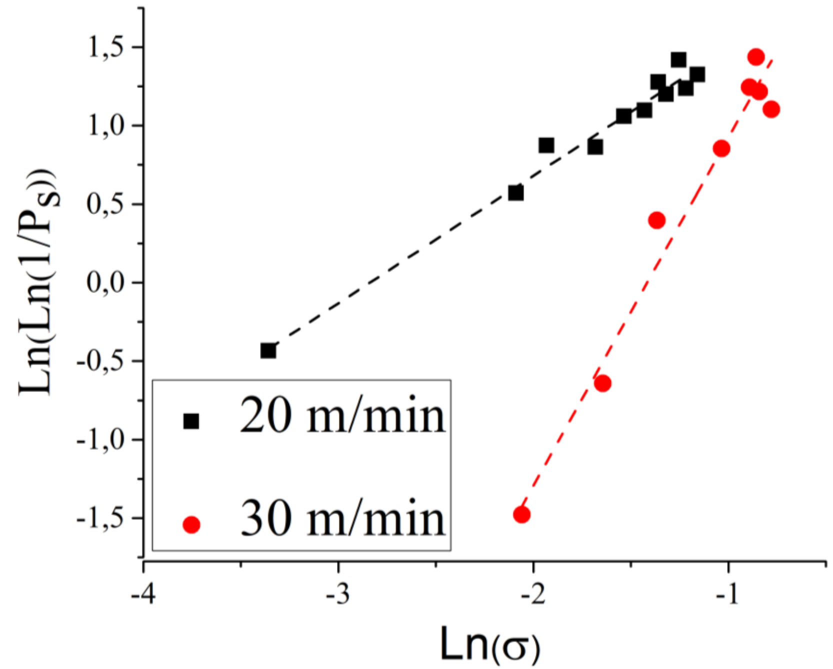

The progressive alignment upon stretching follows a Weibull distribution with axial stress, i.e. non-cooperative loading

Fernández-Toribio et al, in preparation

Elastoplastic deformation

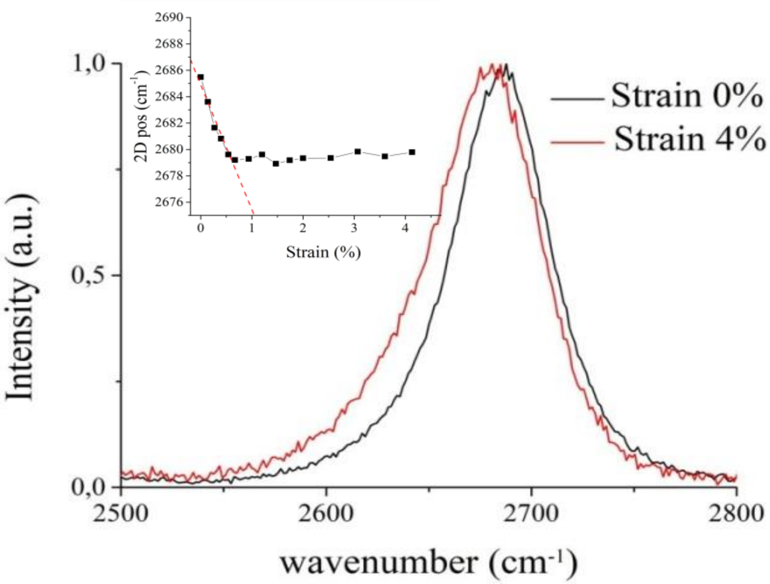

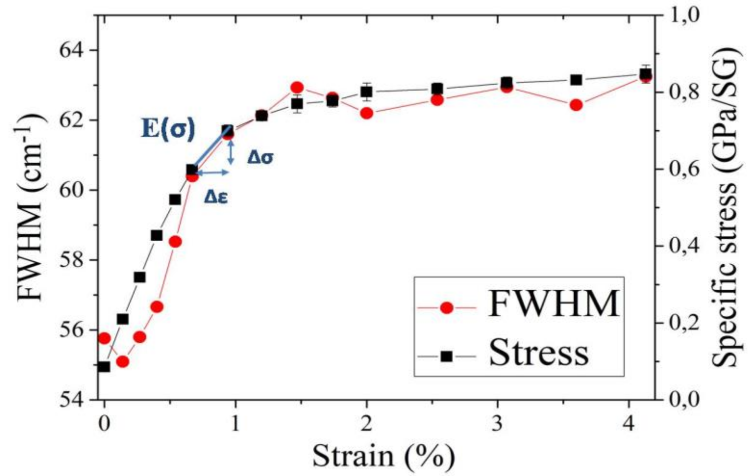

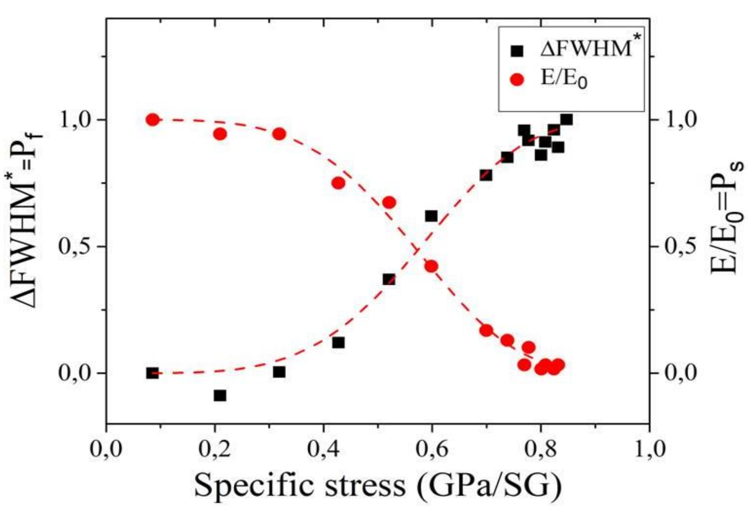

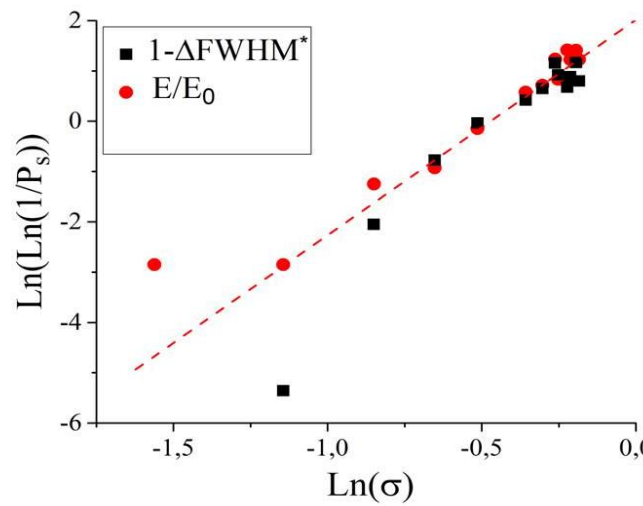

Fernández-Toribio et al, in preparation

Parameters extracted from the analysis

Type of fibre	m (WAXS/SAXS)	m (Raman)	τ_b (MPa)
CNT fibre (20m/min)	0.8	4.3	22.4
CNT fibre (30/min)	2.2	-	40.8

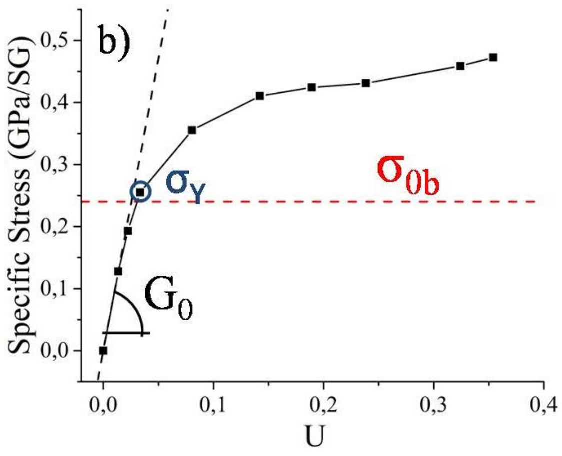

$$\tau_b = \sigma_y \cdot < \sin\phi_y \cdot \cos\phi_y >$$

Next parameters to introduce in the model:

- Stress transfer length
- Lateral CNT packing

A fundamentally different type of carbon material

CNT Fibre

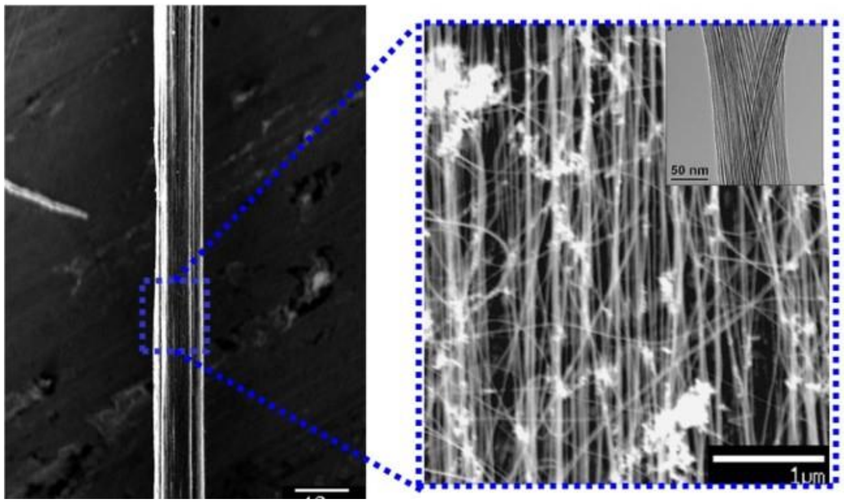

Conductivity 10^3 S/cm

Carbon Fibre

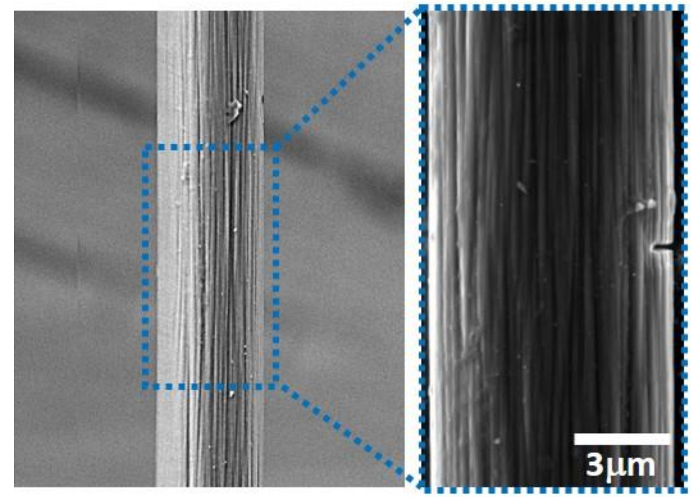

10^2 S/cm

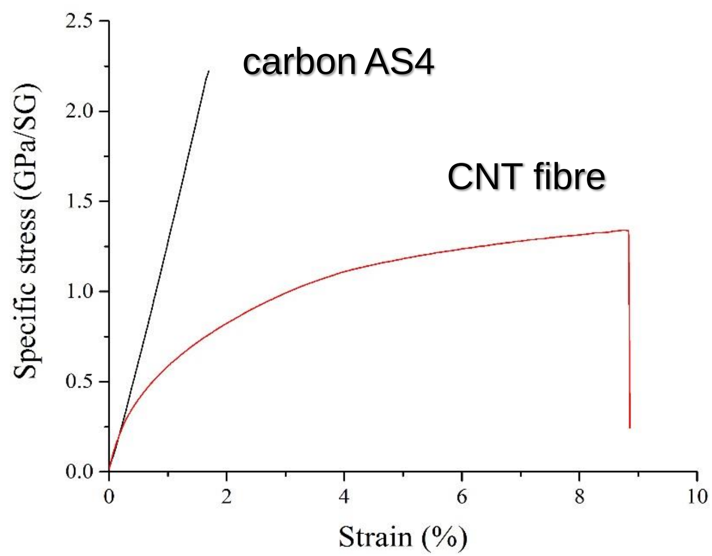

Molecular perfection is decoupled from packing into crystalline domains

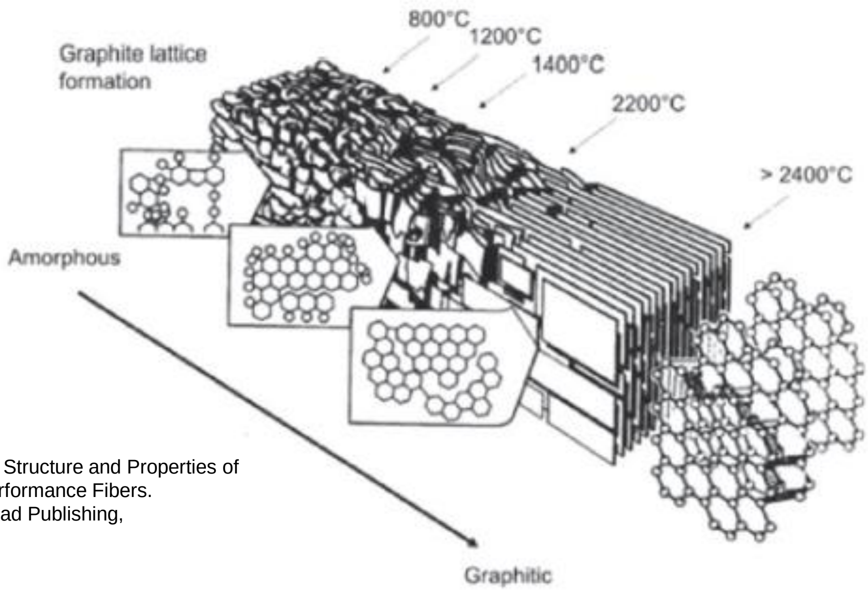

G. Bhat, Structure and Properties of High-Performance Fibers. Woodhead Publishing, 2016.

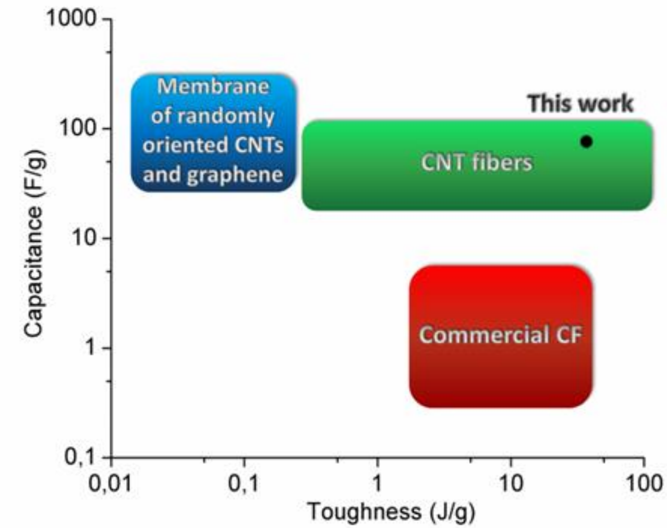

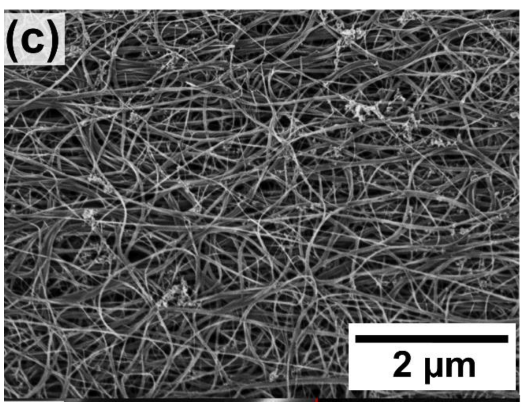

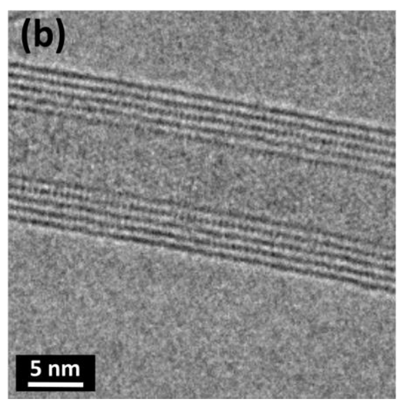

Low dimensional properties

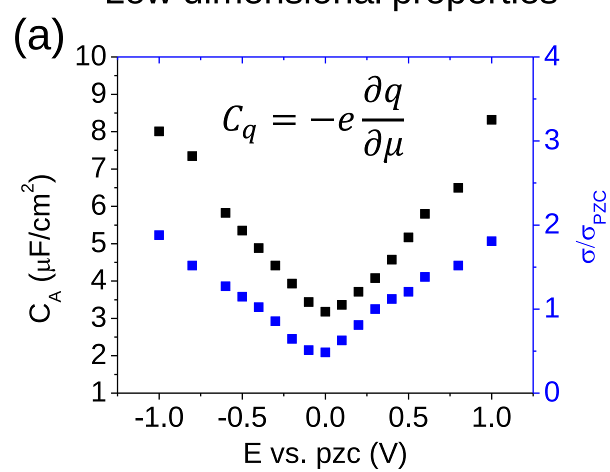

Senokos et al, Nanoscale 8, 3620, 2016

Sensitivity to liquid and gas molecules

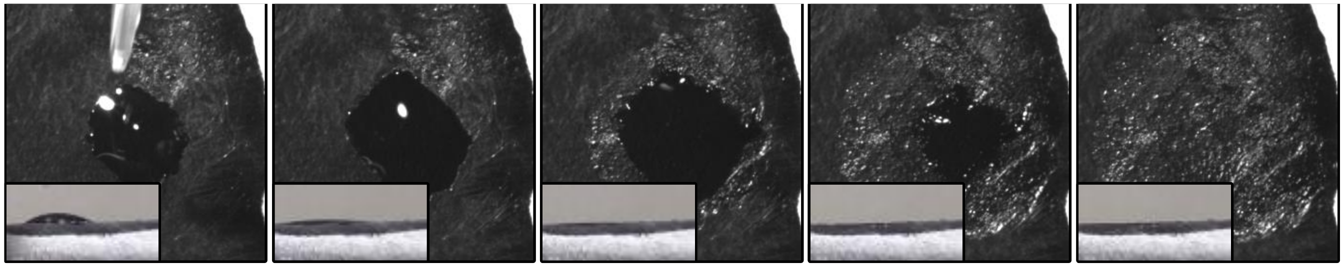

0s 5s 50s 100s 150s

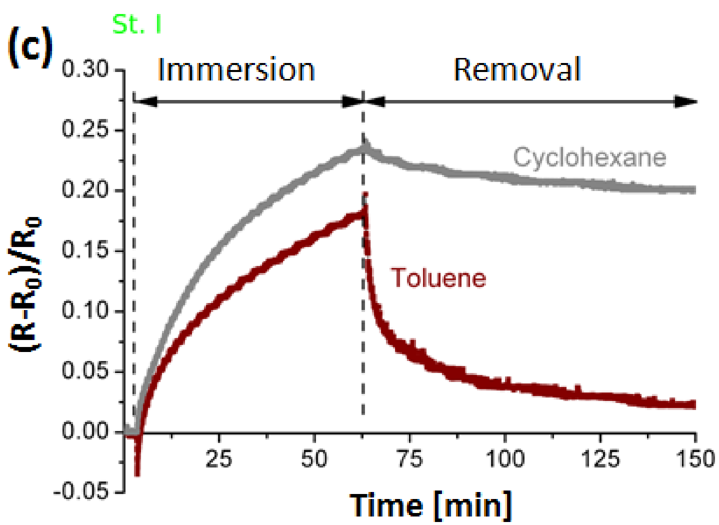

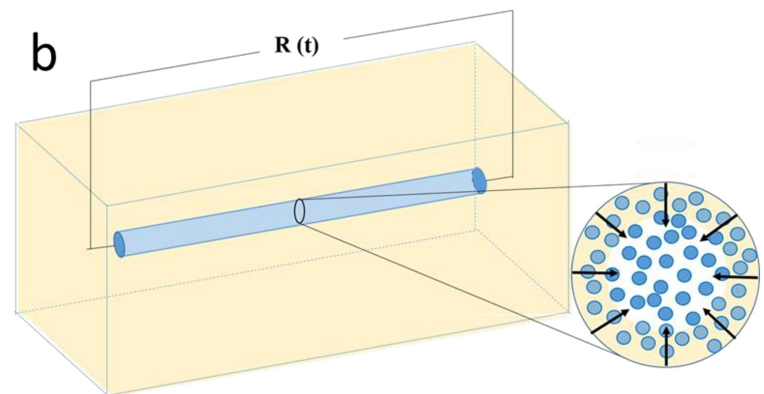

ACS Nano, 7, 8412, 2013

Kinetics of resistance change

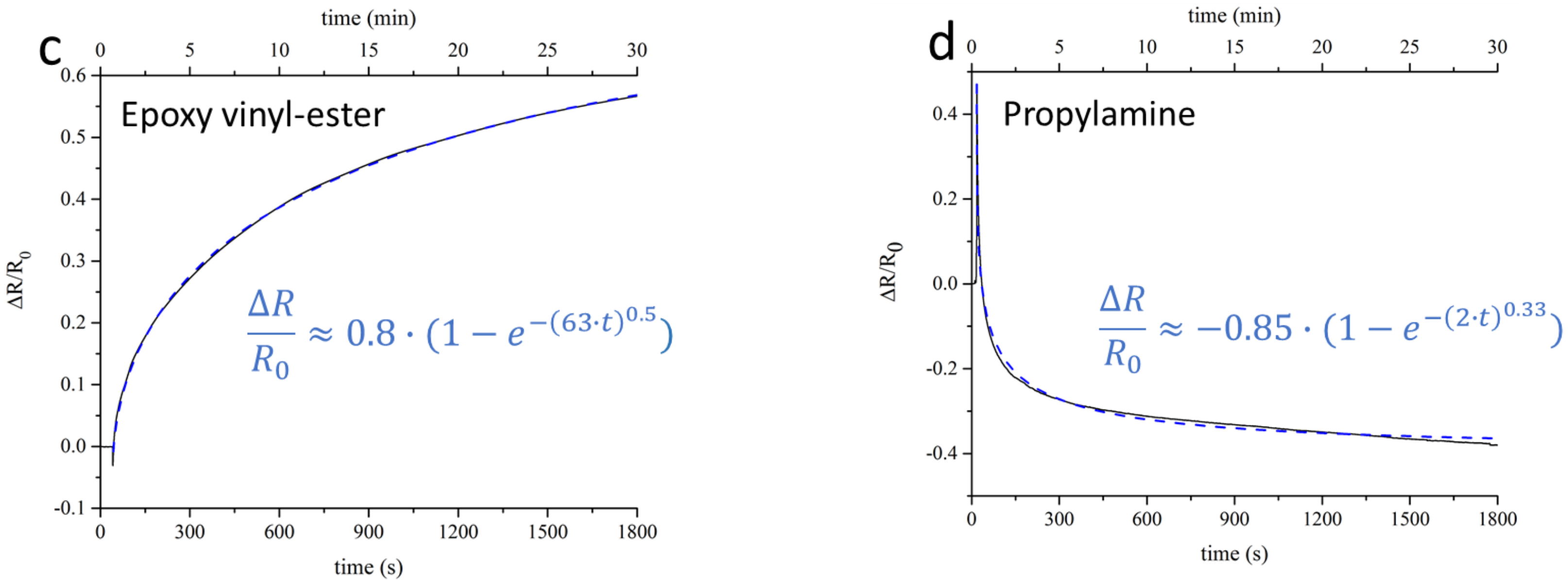

$$\Delta R \approx \Delta R^* \left(1 - e^{-\sqrt{\mathfrak{D} \cdot t}}\right)$$

Kinetics of polymer adsorption

$$\frac{\Gamma(t)}{\Gamma_\infty} \sim \left(1 - e^{-(t/\tau)^\beta}\right)$$

Fernández et al, Adv. Funct. Mater. 2016, 26(39), 1616-3028

Sensor calibration

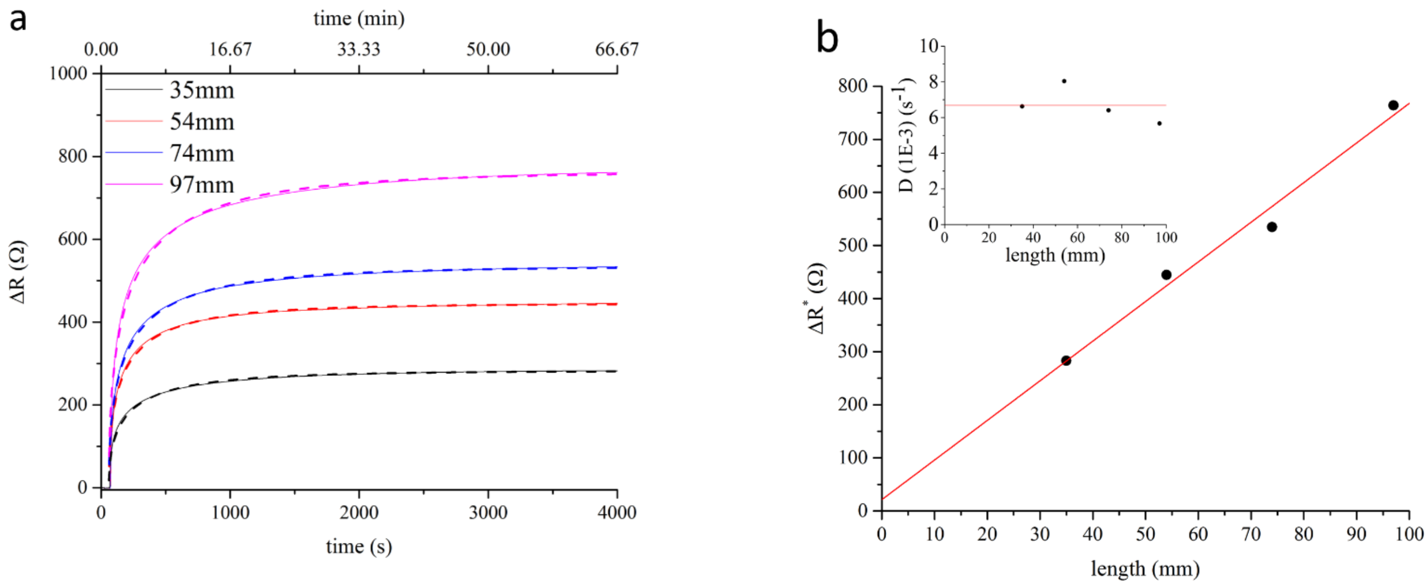

Infiltration of vinyl ester

With this information, it is possible to predict longitudinal flow

$$l(t) = R(t) * \frac{C}{1 - e^{-\sqrt{\mathfrak{D} * t}}}$$

Chemoresistive gauge factor

Vacuum infusion process

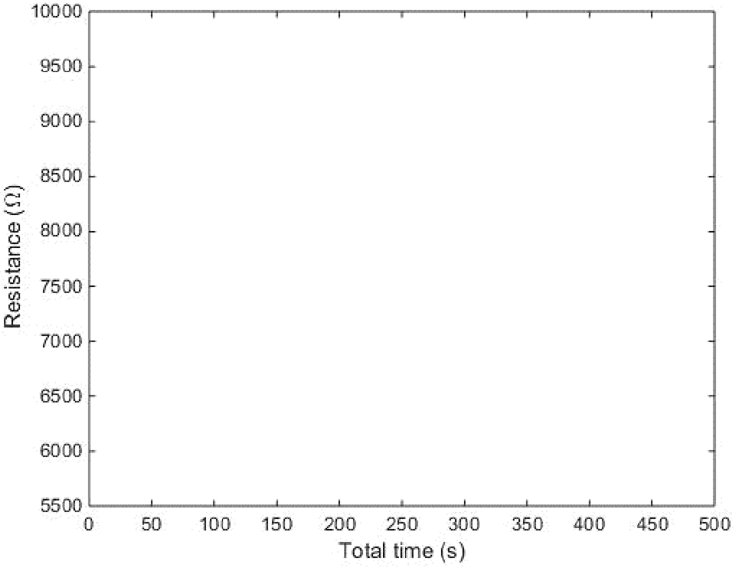

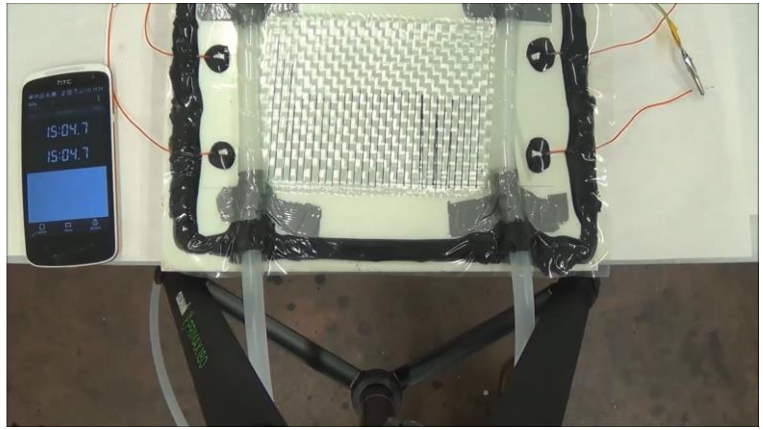
15:04.7
15:04.7

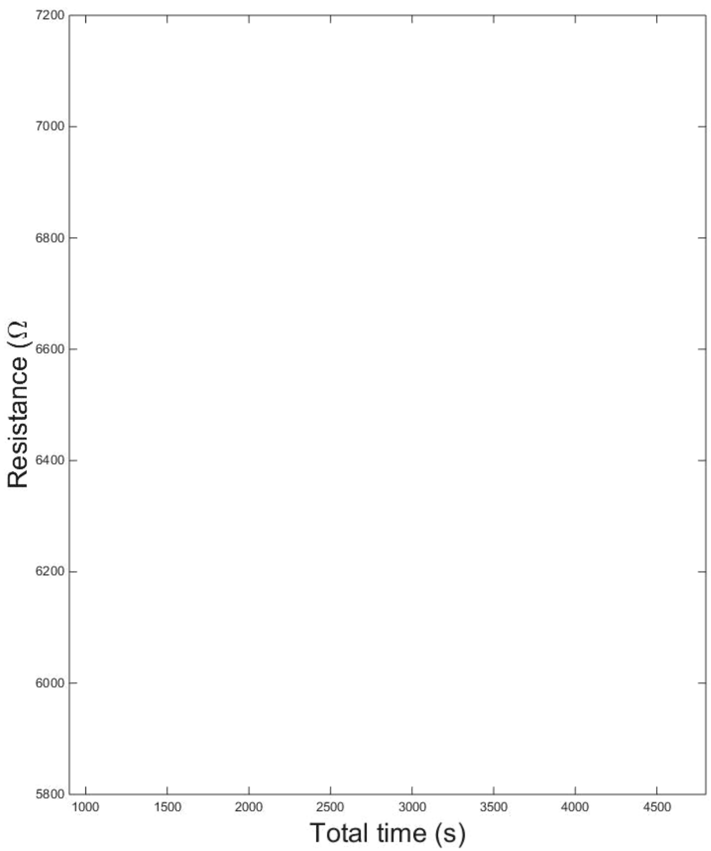
Resistance (Ω)
Total time (s)
7200
7000
6800
6600
6400
6200
6000
5800
1000
1500
2000
2500
3000
3500
4000
4500

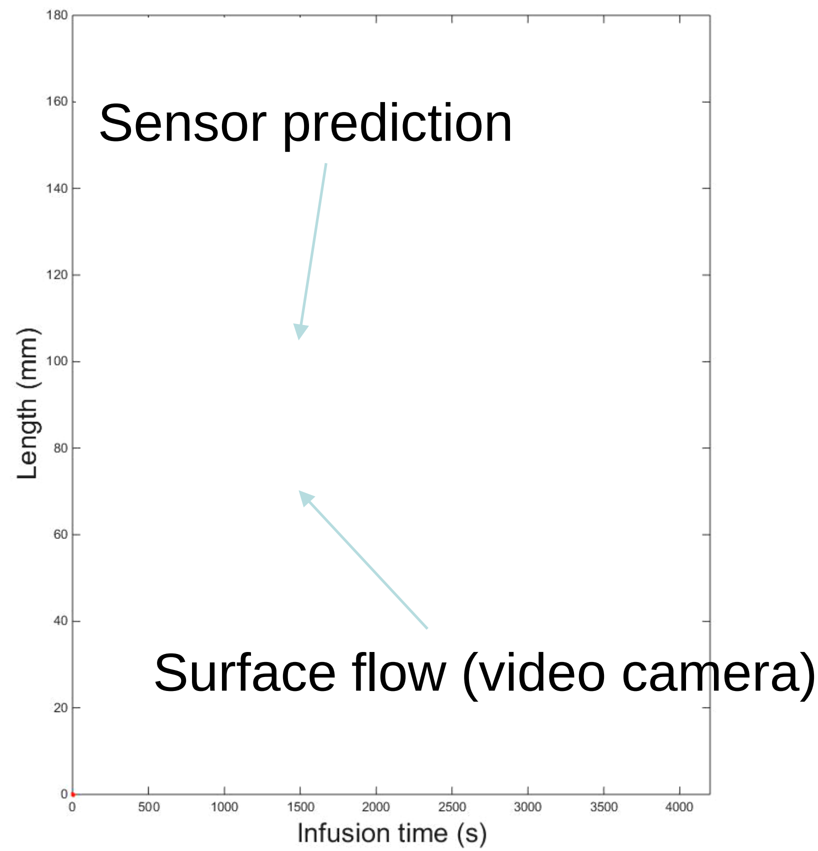
Sensor prediction
Surface flow (video camera)
Length (mm)
Infusion time (s)
180
160
140
120
100
80
60
40
20
0
0
500
1000
1500
2000
2500
3000
3500
4000

Polymer flow sensor during vacuum infusion

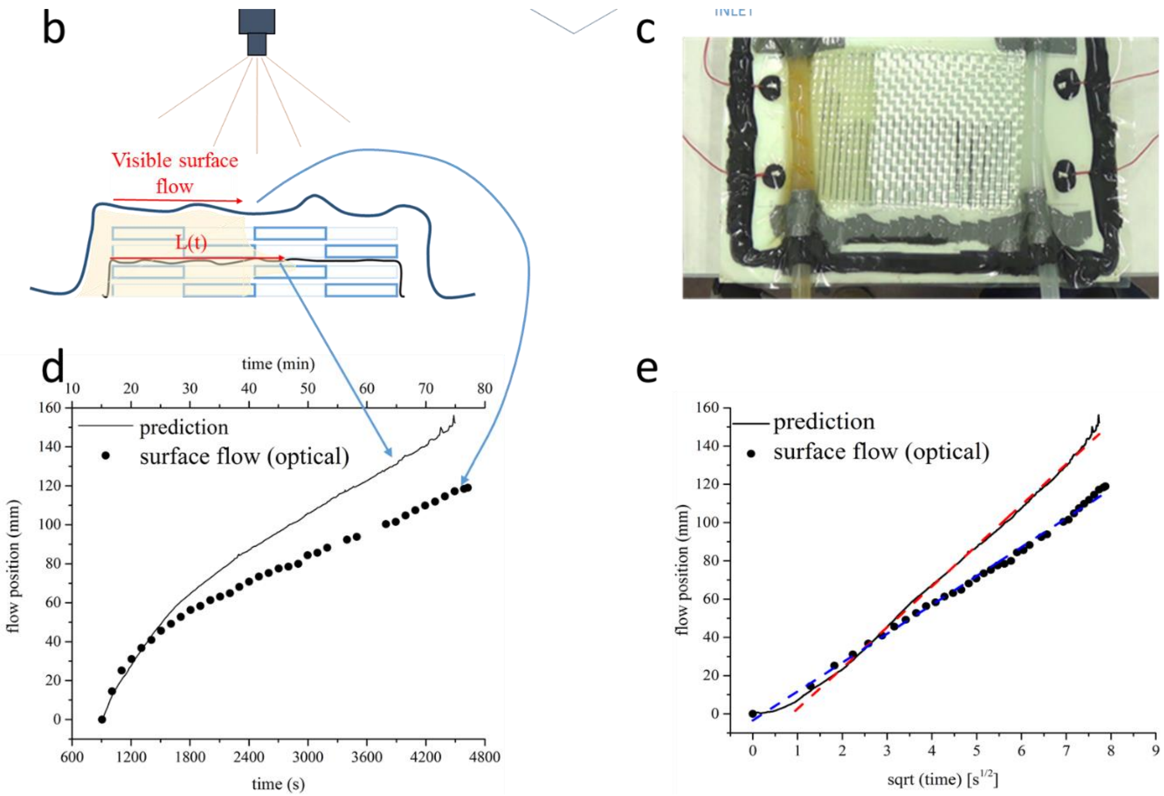

Darcy's law

$$l(t) = \sqrt{\frac{2kP_{atm}}{\eta} t}$$

CNT fibre materials are the ultimate current collector

a)

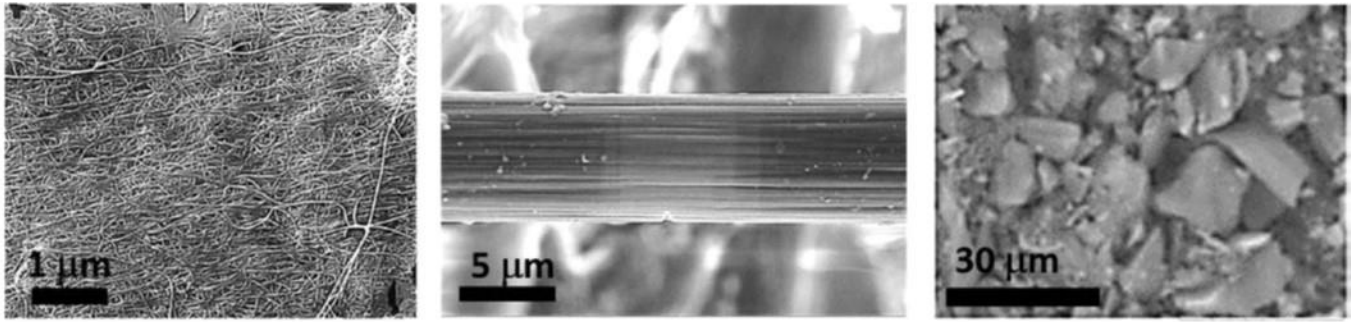

8x10⁵ S/m (longitudinal) | 6x10⁴ S/m (longitudinal) | 10³- 10⁴ S/m

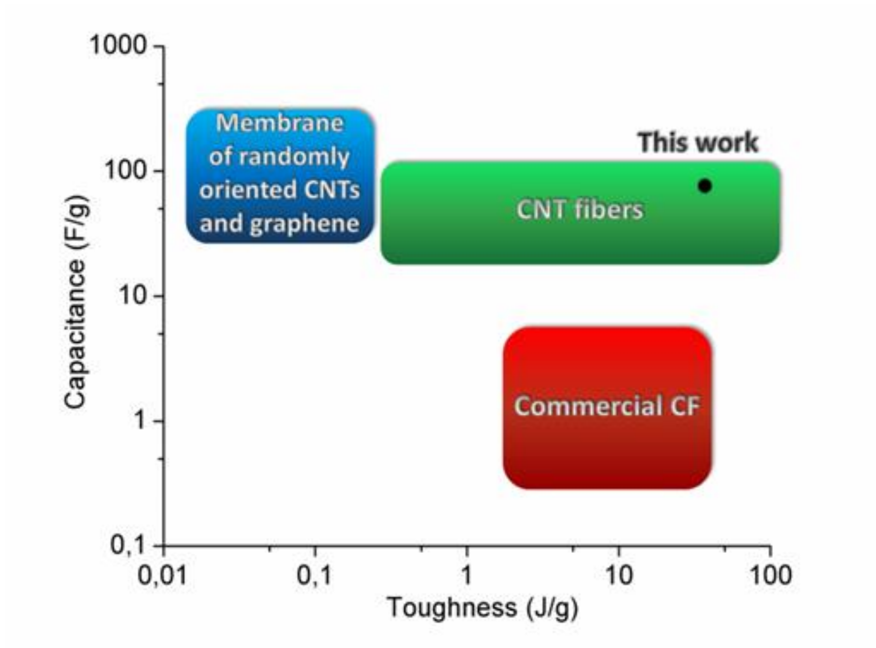

Senokos et al, Nanoscale 8, 3620, 2016

Some examples of applications

Electrode in supercapacitors

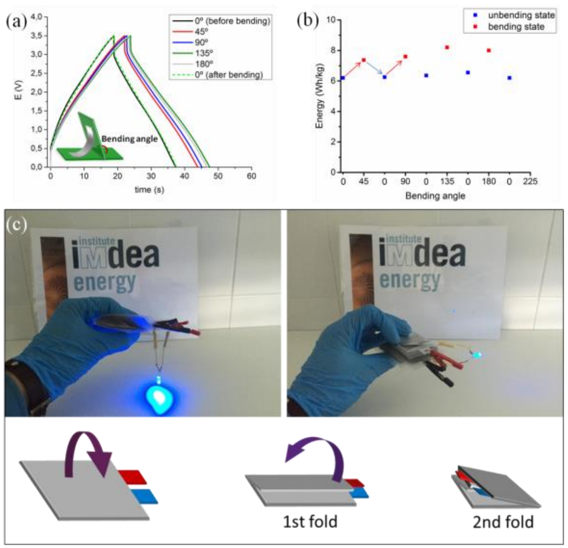

Senokos et al, Adv. Mater. Technol. 2017 1600290

Electrode for ORR and OER in Zn-air battery

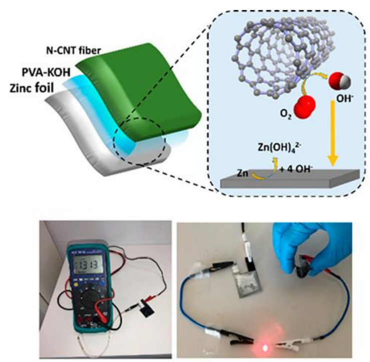

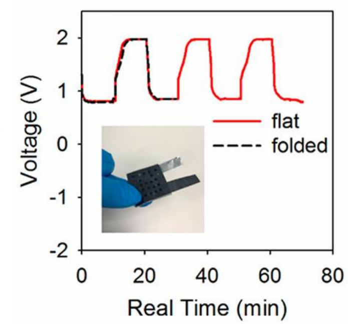

Pendashteh et al; ACS Applied Energy Materials; 2018, 1, 2434

Lighter, tough LIB electrodes

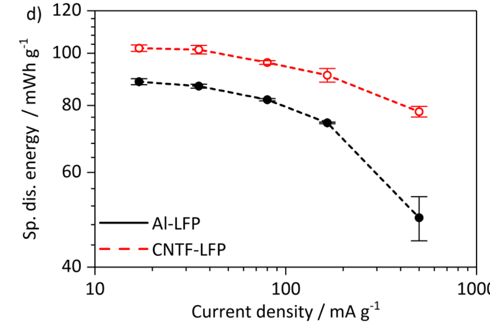

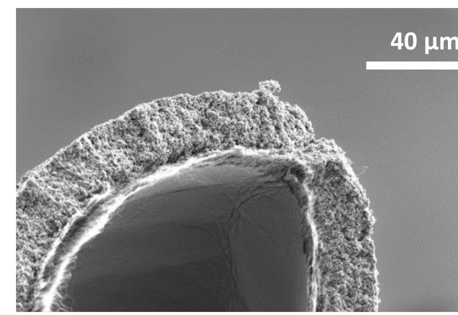

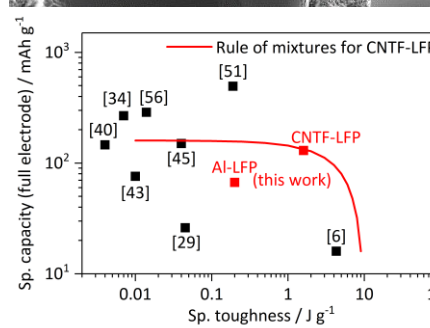

Boaretto et al; DOI:10.1021/acsaem.9b00906

Large-area CNT fibre/MOx hybrids

Conceptually similar to a mesoporous semiconductor electrodes with a built-in current collector

Hybrids with inorganics: TiO_2, ZnO, MnO_2, MoS_2, Cu, V_2O_5, etc

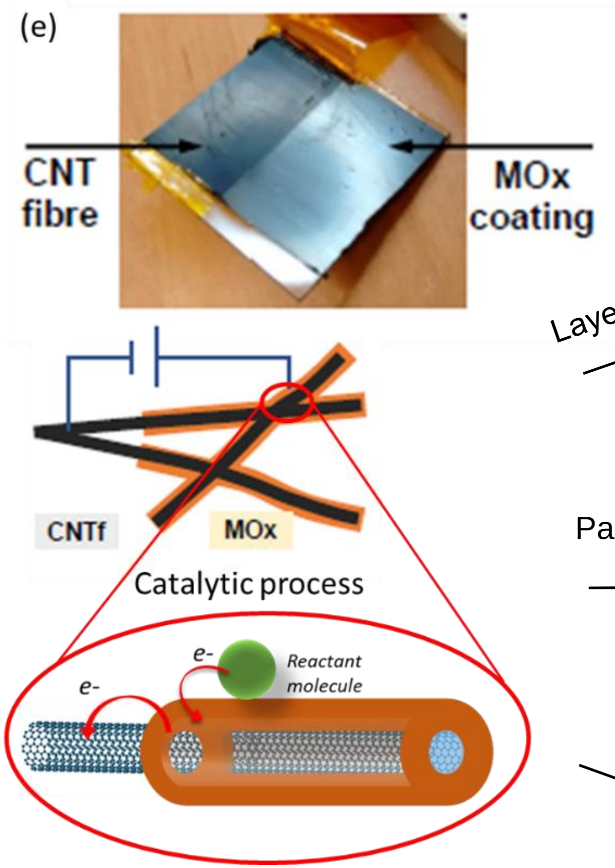

Layered (hydrothermal sol-gel)

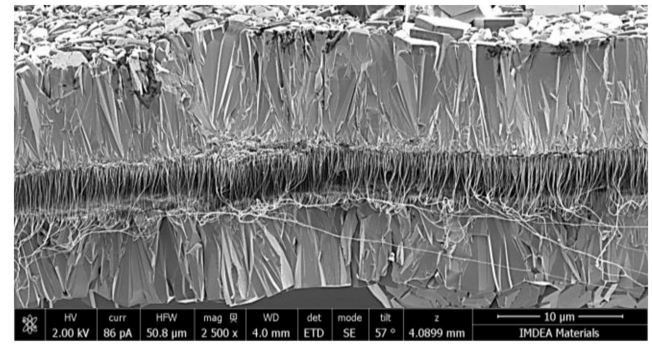

Particulate (electrochemical)

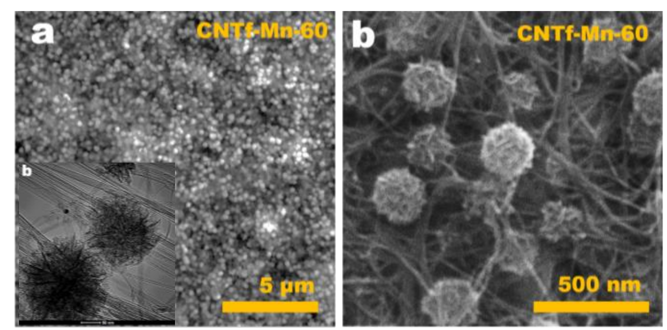

Conformal (ALD)

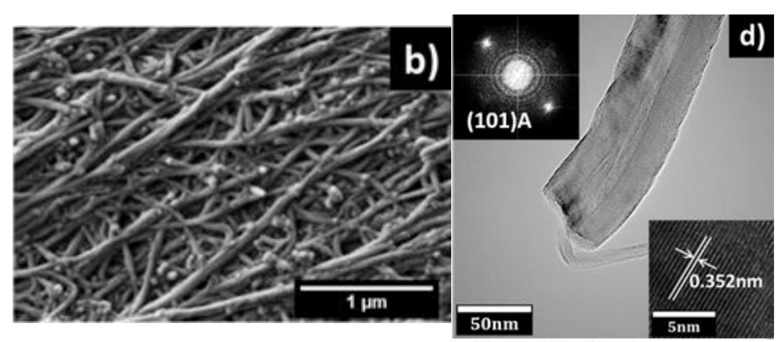

Chapter in Nanocarbons and their hybrids: from synthesis to applications, 2019, Wiley

Current collector for batteries

Coating with active material (LFP)

CNTf sheets before coating

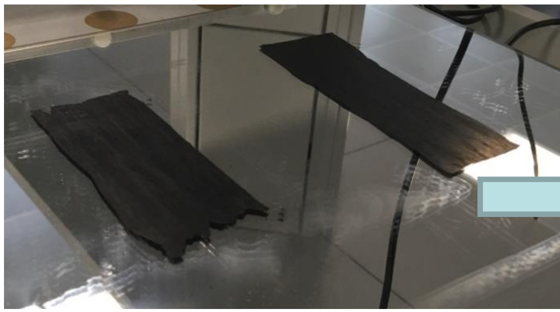

Dried electrodes

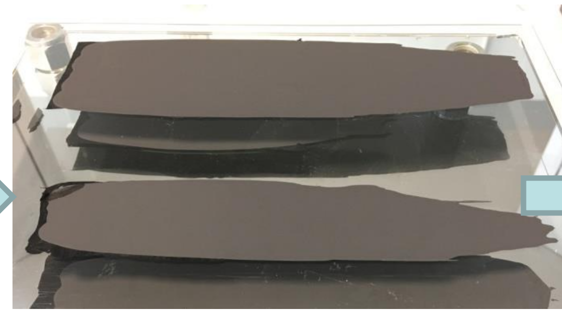

Full electrodes (for pouch cells)

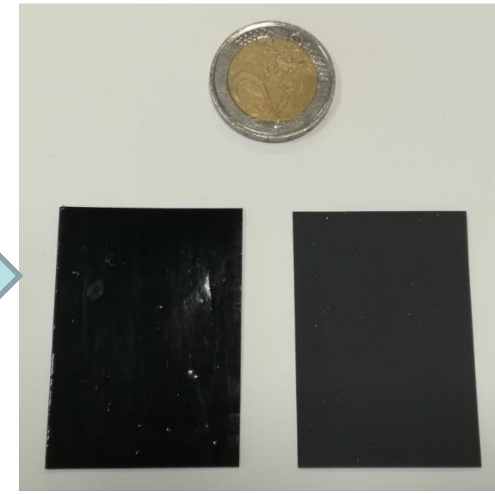

	Thickness / µm	Density / g cm^{-3}
Al	18	2.7
CNTf	10	0.3

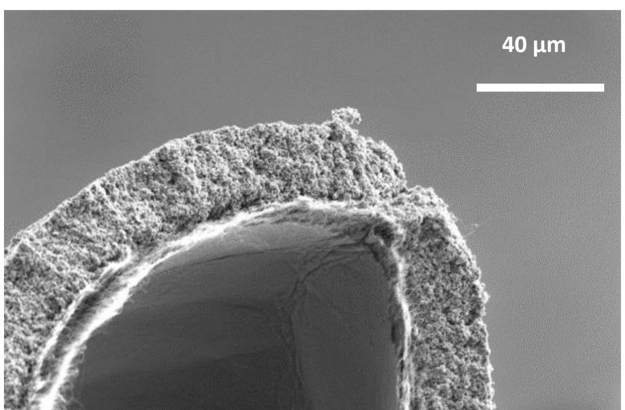

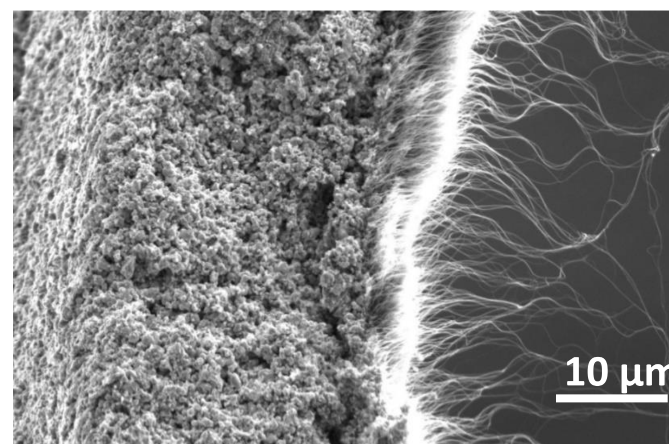

Boaretto et al, DOI:10.1021/acsaem.9b00906

CNTf-based electrodes – Mechanical properties

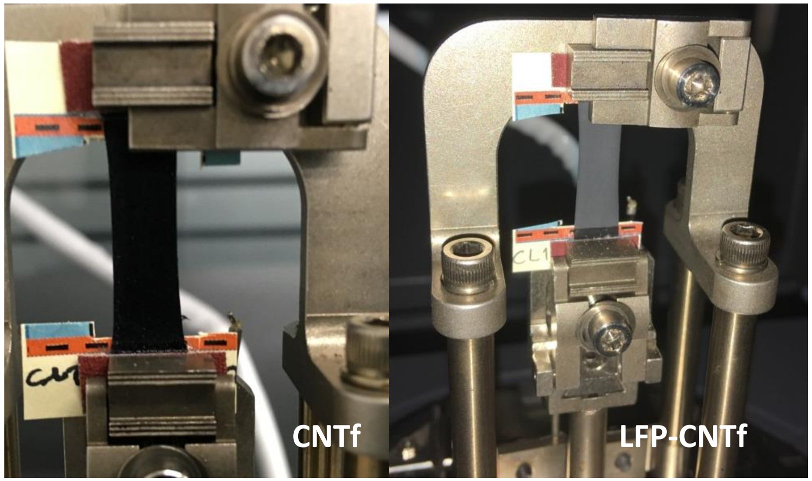

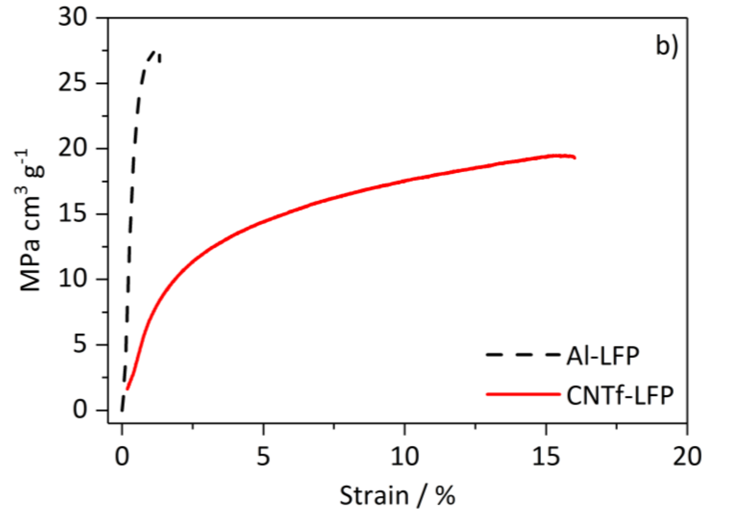

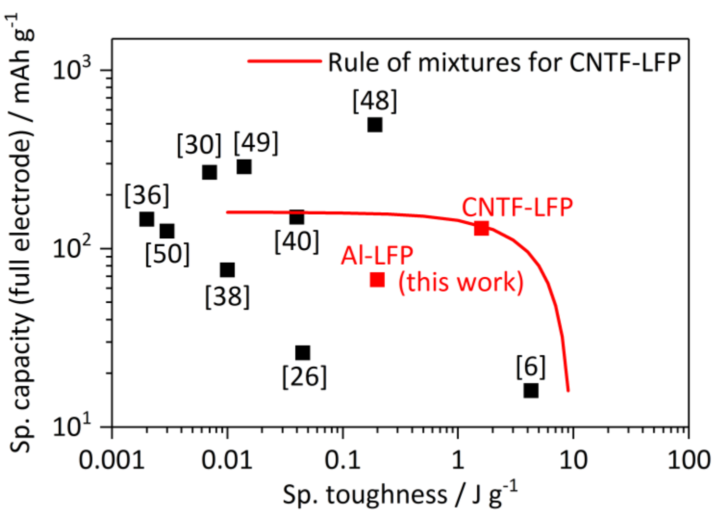

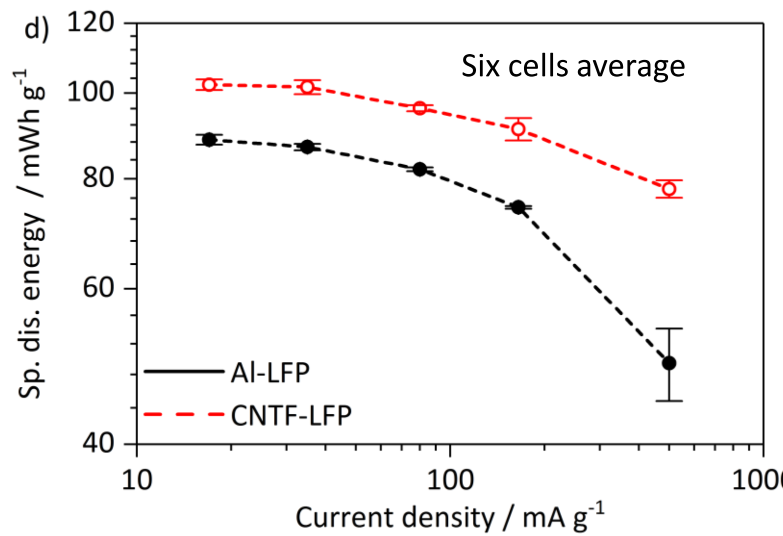

Boaretto et al, under review

Complex, irregular structure

CNT fibres produced by different methods

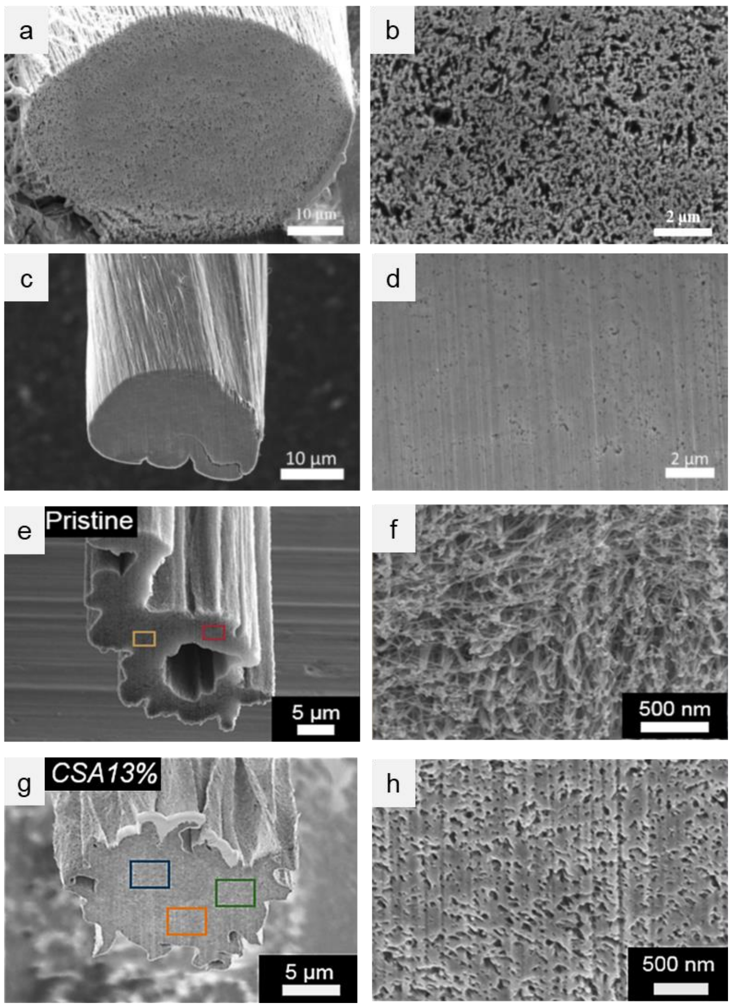

CNT fibres at different length-scales

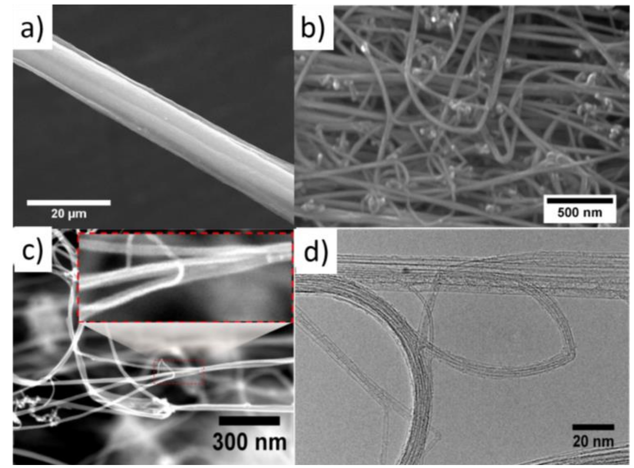

It is a challenge to characterise this structure

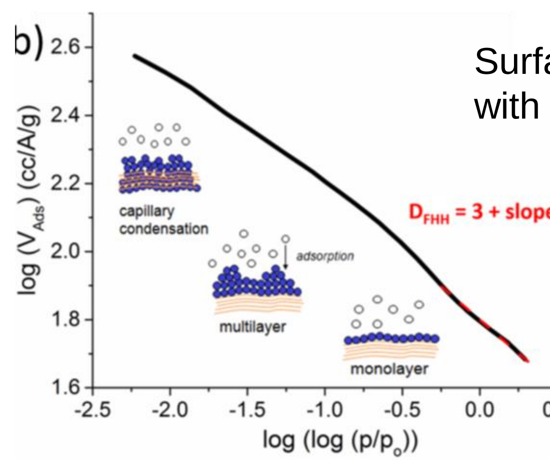

Surface fractal, with D = 2.5

Yue et al, Carbon, 122, 47, 2017

Characterisation of irregular structure by SAXS

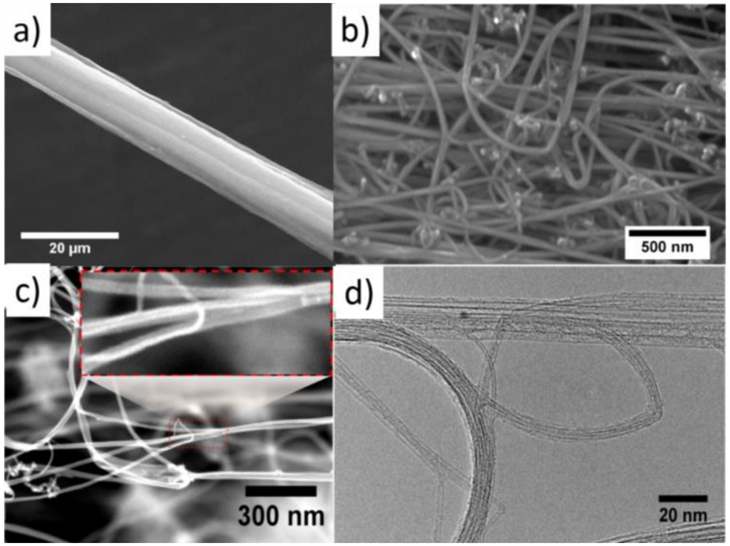

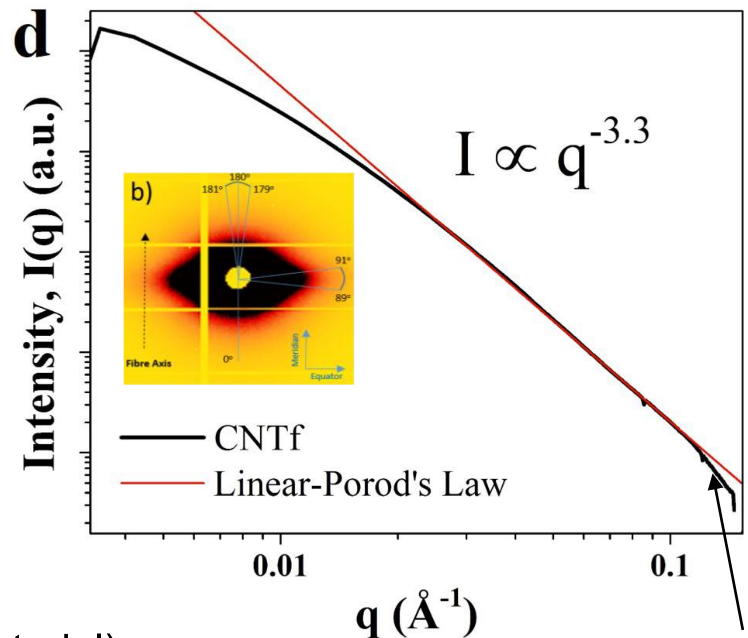

Non-integer Porod exponent (rough, “fractal” material)

Surface to volume ratio

$$K_p = \lim_{q \to \infty} q^4 I(q) = 2\pi(\Delta\rho)^2 Sv$$

Porosity (wrt Bernal graphite)

$$Q = 8\pi(\Delta\rho)^2 P(1-P)$$

$$L_p = \frac{Q}{K_p}$$

Coherence length along cross-section

$$1/L_p = 1/l_{pore} + 1/l_{bundle}$$

Density fluctuations

$$I_{obs} = I_{pores} + I_{DF} + \ldots$$

$$I_{DF} = b_2 q^{-2}$$

Glassy Carbon

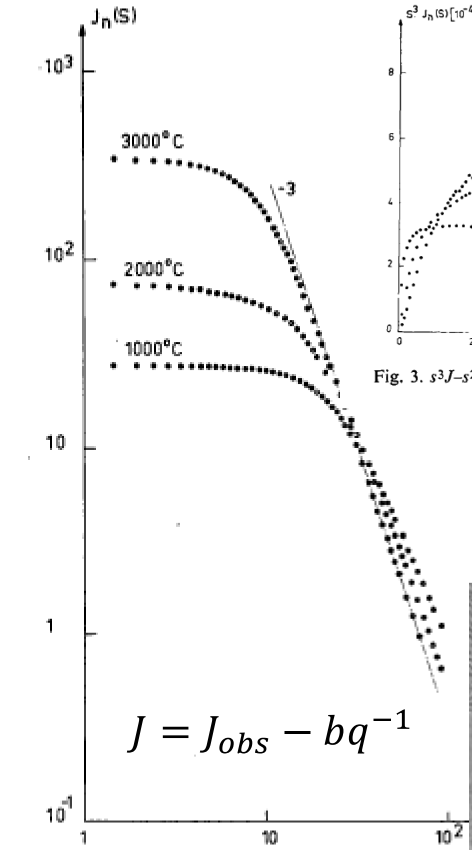

$$J = J_{obs} - bq^{-1}$$

Fig. 1. log J–log s plots for a heat-treatment carbons (LMSC).

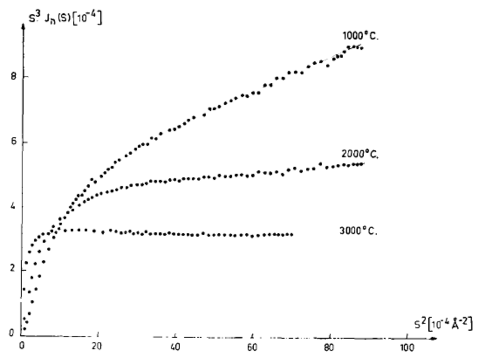

Fig. 3. s^3J–s^2 plots for a heat-treatment series of glassy carbons (LMSC).

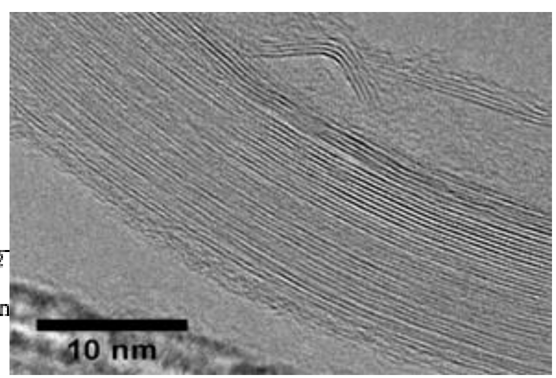

CNT fibre

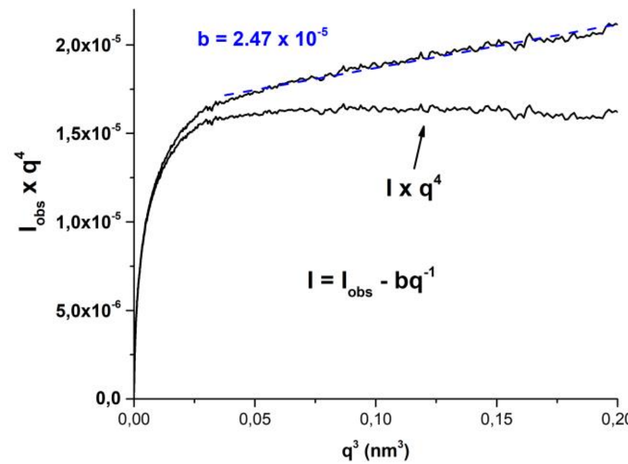

BNNT, National Research Council Canada

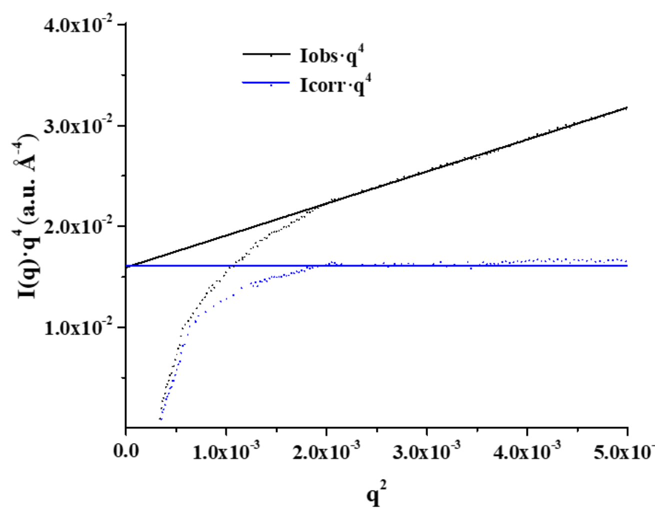

Perret and Ruland, *J. Appl. Cryst.* (1972). 5, 183

Structural parmeters after DF correction

Material	Porod slope	DFs	Porosity	l_{pore} (Å)	l_{bundle} (Å)	Sv (m^2/cm^3)	SSA (m^2/g)
SWCNTF	-4.0	0	0.7	205	89	136	656
CNTF (3-5 layers)	-3.34	1.913	0.66	305	161	85	259.0
MWCNTs Bucky	-3.30	1.91	0.78	552	160	56.1	701.6
CF (PAN, MP)	-3.3, -4	0 – 0-012	0.097-0.33	6-17	36-124	0 - 680	0-367
BNNT	-3.21	2.10	0.81	591	139	54.8	148.1

$$\mathrm{DFs} = \frac{8\pi^2 b_2 P}{a_3 Q} = \frac{\langle \Delta^2 a_3 \rangle}{\langle a_3 \rangle^2} + \frac{\langle \Delta^2 L \rangle}{\langle L \rangle^2}$$

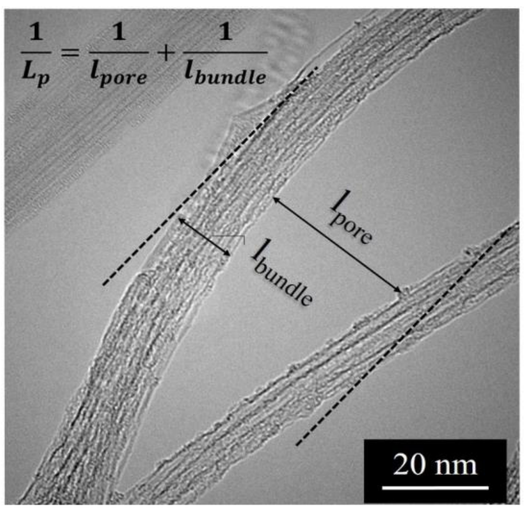

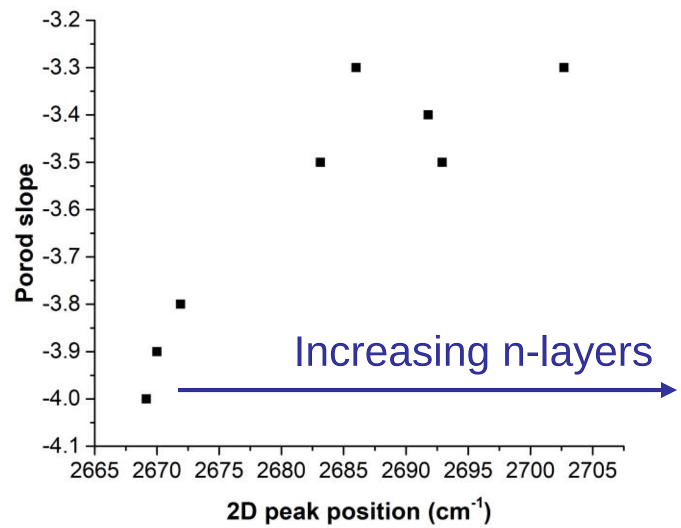

The variations in graphitic spacing and stack size increase with increasing number of layers, producing “coupling of the disorder of lateral fluctuations to the pore structure” Carbon 123 (2017)

Santos et al, J. Mater. Chem. A, 7, 5305, 2019

In-situ vs ex-situ monitoring of pore/bundle structure during electrochemical swelling

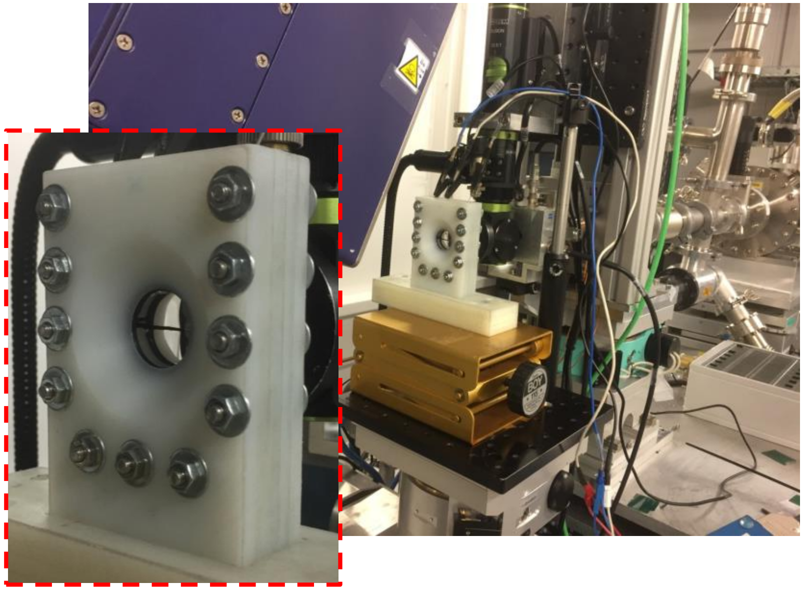

At -3.5 V wrt SHE in $PYR_{14}TFSI$

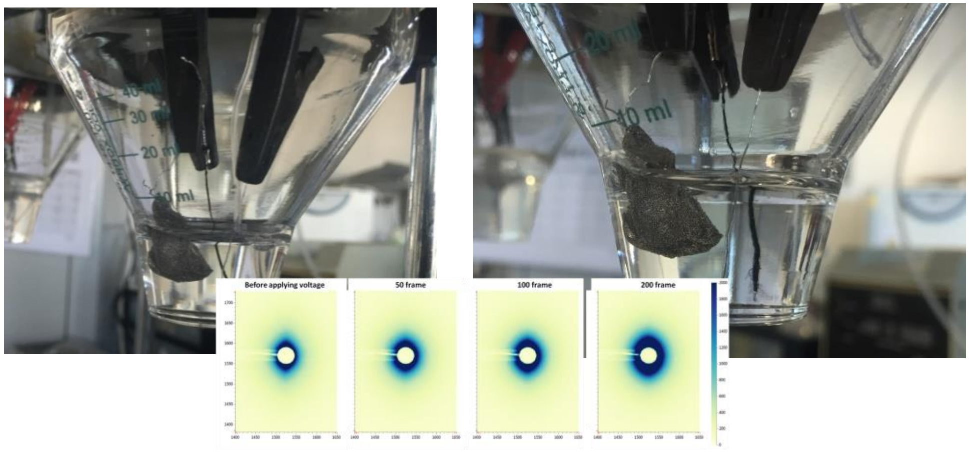

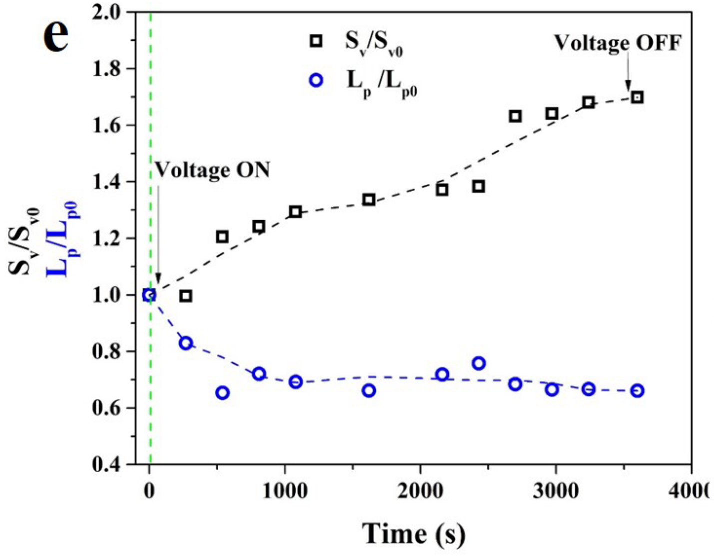

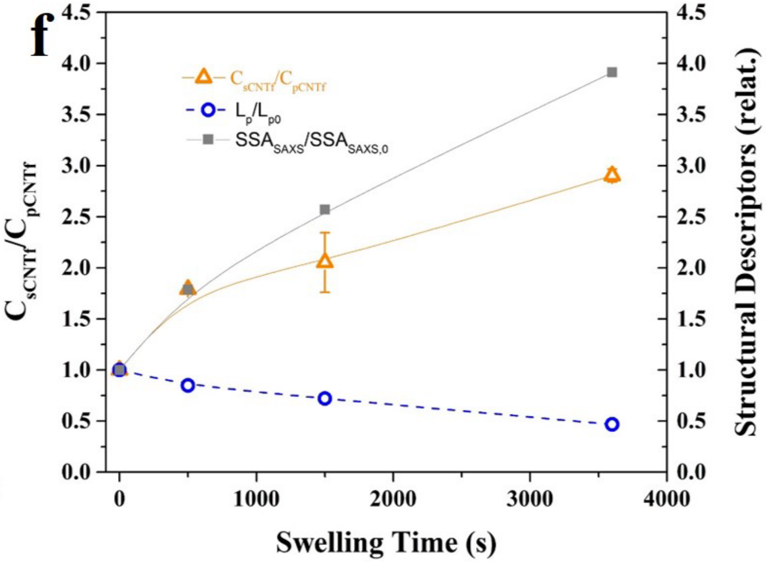

Summary

- CNT fibres can be best described as molecular solids, or graphitic systems with Decoupled crystallinity parallel/perpendicular to basal plane.

- Their tensile properties can be described by the USM and a Weibull distribution of stress distribution through the cross section, with alignment dominating over composition

- CNT fibres are interesting piezo and chemo resistive sensors

- CNT fibres are ideal current collectors for energy storage and transfer.


ELSEVIER
Carbon
Volume 150, September 2019, Pages 191-215

A perspective on high-performance CNT fibres for structural composites

Anastasiia Mikhalchan, Juan José Vilatela

⊞ Show more

https://doi.org/10.1016/j.carbon.2019.04.113

Get rights and content

institute IMDEA materials

Thank you

MNG
Multifunctional Nanocomposites Group

@MNGMaterials

Collaborators:

Carlos González
Rubén Costa
Álvaro Ridruejo
Federico Sket
De-Yi Wang

instituto IMDEA energía

Rebeca Marcilla
Jesús Palma
Enrique García
(IMDEA Energy)

Emilio Pérez
Dani Granados
(IMDEA Nanoscience)

Clean Sky 2

SORCERER
Structural pOweR CompositEs foR futurE civil aircraft

erc European Research Council

La Suma de Todos
Comunidad de Madrid

Gobierno de España
Ministerio de Economía y Competitividad

Air Force Office of Scientific Research
United States Air Force